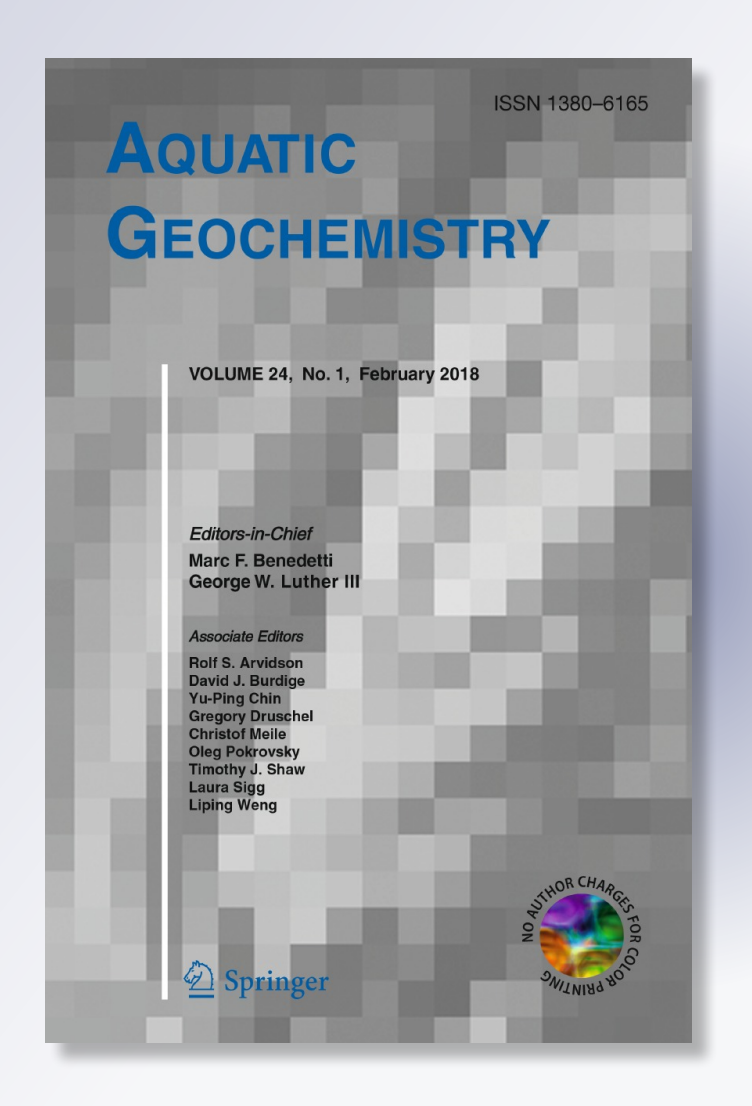
Seasonal Variability of Mineral Formation in Microbial Mats Subjected to Drying and Wetting Cycles in Alkaline and Hypersaline Sedimentary Environments

Ó. Cabestrero, M. E. Sanz-Montero, L. Arregui, S. Serrano & P. T. Visscher

Aquatic Geochemistry

ISSN 1380-6165 Volume 24 Number 1

Aquat Geochem (2018) 24:79-105 DOI 10.1007/s10498-018-9333-2





Your article is protected by copyright and all rights are held exclusively by Springer Science+Business Media B.V., part of Springer Nature. This e-offprint is for personal use only and shall not be self-archived in electronic repositories. If you wish to self-archive your article, please use the accepted manuscript version for posting on your own website. You may further deposit the accepted manuscript version in any repository, provided it is only made publicly available 12 months after official publication or later and provided acknowledgement is given to the original source of publication and a link is inserted to the published article on Springer's website. The link must be accompanied by the following text: "The final publication is available at link.springer.com".





Seasonal Variability of Mineral Formation in Microbial Mats Subjected to Drying and Wetting Cycles in Alkaline and Hypersaline Sedimentary Environments

Ó. Cabestrero¹ · M. E. Sanz-Montero¹ · L. Arregui² · S. Serrano² · P. T. Visscher³

Received: 21 December 2017 / Accepted: 19 February 2018 / Published online: 23 February 2018 © Springer Science+Business Media B.V., part of Springer Nature 2018

Abstract Interactions of the microbial mat community with the sedimentary environment were evaluated in two shallow, ephemeral lakes with markedly different hydrochemistry and mineralogy. The characterization of growing and decaying microbial mats by light microscopy observations and fluorescence in situ hybridization was complemented with biogeochemical and mineralogical measurements. The lakes studied were Eras and Altillo Chica, both located in Central Spain and representing poly-extreme environments. Lake Eras is a highly alkaline, brackish to saline lake containing a high concentration of chloride, and in which the carbonate concentration exceeds the sulfate concentration. The presence of magnesium is crucial for the precipitation of hydromagnesite in microbialites of this lake. Altillo Chica is a mesosaline to hypersaline playa lake with high concentrations of sulfate and chloride, favoring the formation of gypsum microbialites. Differences in the microbial community composition and mineralogy of the microbialites between the two lakes were primarily controlled by alkalinity and salinity. Lake Eras was dominated by the cyanobacterial genus Oscillatoria, as well as Alphaproteobacteria, Gammaproteobacteria and Firmicutes. When the mat decayed, Alphaproteobacteria and Deltaproteobacteria increased and became the dominant heterotrophs, as opposed to Firmicutes. In contrast, Deltaproteobacteria was the most abundant group in Lake Altillo Chica, where desiccation led to mats decay during evaporite formation. In addition to Deltaproteobacteria, Cyanobacteria, Actinobacteria, Alphaproteobacteria and Gammaproteobacteria were found in Altillo Chica, mostly during microbial mats growth. At both sites, microbial mats favored the precipitation of sulfate and carbonate minerals. The precipitation of carbonate is higher in the soda lake due to a stronger alkalinity engine and probably a higher degradation rate

Department of Marine Sciences, University of Connecticut, Groton, CT 06340, USA



Department of Petrology and Geochemistry, Faculty of Geological Sciences, Complutense University of Madrid, José Antonio Novais, 12, 28040 Madrid, Spain

Department of Microbiology, Faculty of Biological Sciences, Complutense University of Madrid, José Antonio Novais, 12, 28040 Madrid, Spain

of exopolymeric substances. Our findings clarify the distribution patterns of microbial community composition in ephemeral lakes at the levels of whole communities, which were subjected to environmental conditions similar to those that may have existed during early Earth.

Keywords Playa lakes · Hypersaline · Alkaline · Desiccation · Microbial mats · Seasonality

1 Introduction

Microbes have influenced the formation of minerals and sedimentary rocks such as stromatolites and have affected the global biogeochemical cycles since they first appeared on Earth (Newman and Banfield 2002). Specifically, halophilic and alkaliphilic organisms may have existed early during Earth's history when hypersaline, high pH conditions may have prevailed (Jones et al. 1998; Yang et al. 2016).

There is increasing evidence that microbes forming microbial mats proliferate in playa lakes, i.e., intracontinental, small, shallow basins, which frequently evaporate to dryness (Power et al. 2007; Navarro et al. 2009; Foster et al. 2010; Sanz-Montero and Rodríguez-Aranda 2013; Rodríguez-Aranda and Sanz-Montero 2015; Sanz-Montero et al. Sanz-Montero et al. 2015a, 2016). In these extreme environments with wet-dry cycles, interactions between microorganisms and hydrochemistry play an important role in brine evolution and precipitation of minerals (e.g., carbonates and sulfates) leading to the formation of microbialites (Baumgartner et al. 2006; Cabestrero et al. 2013, 2014a; Farías et al. 2014; Sanz-Montero et al. 2013a, 2015b; Cabestrero and Sanz-Montero 2018). Playa lakes are conspicuous worldwide (Navarro et al. 2009) and harbor a vast number of biogeochemical processes, notably within the sediments. However, few geomicrobiological studies have been carried out in ephemeral playa lakes in which water availability and composition (salinity, pH, Eh, etc.) as well as the mineralogy change drastically through the year.

In this paper, the microbial composition of two distinctive extreme playas lakes, chosen from a total of six playa basins distributed across two evaporitic systems that undergo wet-dry cycles, was investigated. Both lakes are located in hydrologically closed setting at similar latitude and climatic conditions, but with markedly different hydrochemistry and mineralogy (Cabestrero et al. 2015a; Cabestrero and Sanz-Montero 2018). One of these playa lakes, Eras, is a highly alkaline (pH \leq 11.3), brackish to saline, trona-containing system, with a high concentration of chloride and in which the concentration of carbonate ion exceeds sulfate. Unlike other soda lakes, in addition to Na carbonates, Lake Eras is characterized by a high concentration of Mg²⁺ that leads to the formation of Mg carbonates, notably hydromagnesite (Sanz-Montero et al. 2013b). As such, Lake Eras is one of the few modern environments where hydromagnesite is a dominant precipitate in microbialites (Sanz-Montero et al. 2013c). Altillo Chica, in the other playa system, is a mesosaline to hypersaline (2 to > 300 g L^{-1}) lake, with a high concentration of sulfate and chloride, favoring the formation of gypsum microbialites (Sanz-Montero et al. 2015b) with other minerals precipitating in crusts such as Mg and/or Na sulfates (Cabestrero et al. 2013, 2014a; Sanz-Montero et al. 2013a; Cabestrero and Sanz-Montero 2018).

The purpose of this paper is to evaluate the precipitation of the minerals formed in microbial mats present in evaporitic lakes subjected to dry-wet cycles. Permanently submersed mats have been described in detail (Schneider et al. 2013; Wong et al. 2015), but



the reports of mats subjected to dry—wet cycles that grow submerged and decay seasonally are scarce. Experimental treatment of excised mat samples complemented with a molecular diversity study was carried out to investigate mat development, which was used to better define the microbial groups and understand the mechanisms that affect mineral precipitation. In addition, microbial mat layering was correlated to geochemical gradients (e.g., pH, oxygen and sulfide profiles) on a small scale and with the physicochemical and geochemical characteristics (e.g., ions, salinity, temperature, pH, dissolved oxygen (DO) and Eh) on a large spatial scale.

2 Site Description

The playa lakes studied (Eras and Altillo Chica) are found in two different, closed-drainage areas located in the center of Spain, approximately 150 km north (41°12′1.04″N, 4°34′55.73″W) and 100 km south of Madrid (39°42′3.94″N, 3°18′9.97″W), respectively (Fig. 1).

2.1 Lake Eras

Eras (ER) is an alkaline (pH up to 11.3), brackish to saline $(0.4-15.1~{\rm g~L}^{-1})$ and ephemeral lake, located in a closed-drainage area in the Duero Basin, Central Spain (Fig. 1a). Lake Eras with a maximum area of $0.1~{\rm km}^2$ is a groundwater-fed, shallow basin (less than $0.6~{\rm m}$ deep). The basin is located at an elevation of 802 m, overlying Cenozoic siltstones, sandstones, marlstones and eolian sands. The region has a continental climate, characterized by seasonal changes in temperature (from $-10~{\rm to}~38~{\rm ^{\circ}C}$) and in rainfall (wet period during the winter and early spring). The area has low annual precipitation levels (400–500 mm y⁻¹). Lake Eras is usually dry from August to October, when it converts to a playa. Major ions in the lake waters are Na⁺ and Cl⁻, with a Mg²⁺/Ca²⁺ up to 93 and a Na⁺/Cl⁻ ranging from 1.3 to 1.9 (Sanz-Montero et al. 2013b; Cabestrero and Sanz-Montero 2018).

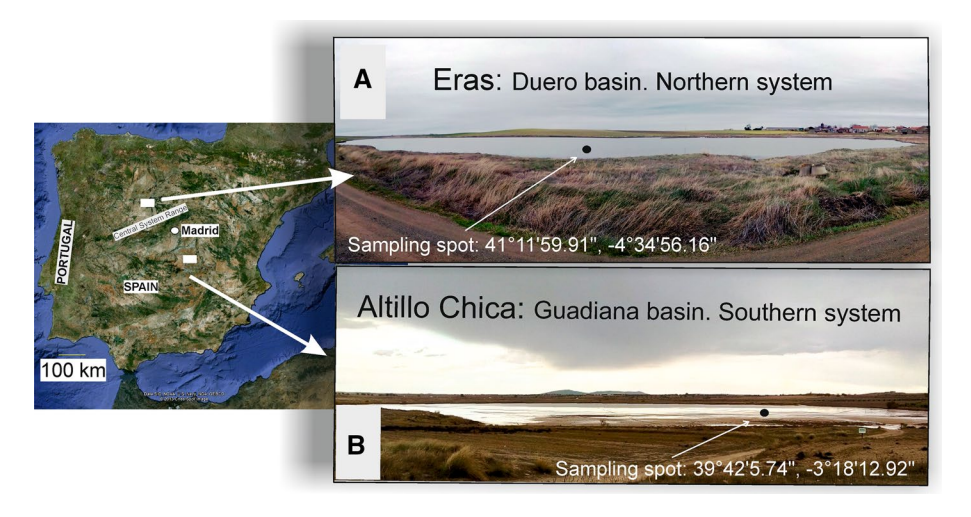


Fig. 1 Location of the study sites in central Spain. Overview images of playa lakes Eras (a) and Altillo Chica (b) in the spring



The muddy sediment of this playa basin comprises up to 50% of detrital grains (clays, feldspars, quartz and carbonates) and authigenic carbonates (hydromagnesite, nesquehonite, dolomite, calcite and locally trona), sulfates (thenardite, hexahydrite, starkeyite, gypsum, among others) and chlorides (Cabestrero and Sanz-Montero 2018).

2.2 Lake Altillo Chica

The hypersaline playa lake Altillo Chica has a surface area of 0.2 km² and is located in a endorheic wetland in La Mancha region, Central Spain (Fig. 1b). The basin has no inflow from rivers, groundwater is negligible, so the lake is fed predominantly by precipitation (Sanz-Montero et al. 2015a). The region has a continental, semiarid climate characterized by a high evaporation (1300–1660 mm yr⁻¹) and low precipitation (360–500 mm yr⁻¹) resulting in saline conditions. During the winter, the nearly horizontal surface in the center of the playa lake is unevenly covered by a thin sheet of water that rarely exceeds 15 cm. A succession of storms in winter erodes the lake bed and moves large volumes of sediments (Sanz-Montero and Rodríguez-Aranda 2013; Sanz-Montero et al. 2015a). During the dry season (May–October), the playa desiccates completely. The wetland is located at an elevation of 681 m superimposed on horizontally bedded Neogene sedimentary rocks consisting of gypsum, chert, carbonates and quarzitic sandstone and conglomerates. The lake water is mesosaline to hypersaline (2–3404 g L⁻¹), with a dominant Mg²⁺–Cl⁻ ionic composition (Cabestrero and Sanz-Montero 2018; Cabestrero et al. 2018).

The bed of Altillo Chica comprises up to 25% of detrital grains and a variety of authigenic minerals. Sulfates are the most abundant precipitates (e.g., lenticular gypsum, hexahydrite, bloedite and a suite of hydrated, Na and Mg sulfates) and with a minor contribution of carbonates (mainly, calcite), halite and Mg clay minerals (Sanz-Montero and Rodríguez-Aranda 2013; Del Buey et al. 2018).

3 Materials and Methods

3.1 Sample Collection

The previous field trips done from 2009 to 2014 showed that the precipitation of some minerals coincided with the presence of microbial mats, mostly from March to May. Accordingly, representative samples of non-lithifying microbial mats were collected at two different stages (two field trips to each basin; Fig. 1), the first during growth of microbial mats and the second when the mats were decaying. Samples also comprised lithified surface layers, carbonate and clay-based sediments in the northern lake (Sanz-Montero et al. 2013b), and gypsum, clay-based sediments in the southern lake (Sanz-Montero and Rodríguez-Aranda 2013; Cabestrero et al. 2014b) and water samples.

An additionally, 15–20 sediment samples were divided into three sets: one set was used for the determination of geological properties using dissecting microscopy (Leica MZ16 with 11.5× magnification) and light and fluorescence light optical microscopy (Olympus BX51). A second set was used for laboratory manipulations with intact mats and for microbial incubations. For these laboratory experiments, samples of 100–200 g were collected and included the upper three layers of each mat (green–yellow, red–brown and gray–black). All samples were stored in the dark at 4 °C until processed. A third set was archived and kept at 4 °C until further analysis. In addition, previously published data (for instance,



mineralogy in winter and summer conditions) and some field observations were used to the design a conceptual model of seasonal cycles.

3.2 Microbial Diversity Analysis

A total of 10 fixed samples (50% ethanol:water (v/v)) and 15 non-fixed replicates were taken from Lake Eras and Lake Altillo Chica. Microscopic observation of photosynthetic protists was carried out within 24 h after sampling. Subsets (25 µl aliquots) of living or stained specimens (silver carbonate impregnation, Fernandez-Galiano 1976) were viewed using bright field, phase contrast (Olympus BX50 with a Canon Power Shot A620 digital camera) and differential interference contrast (DIC) microscopy (Nikon Eclipse 80i with a Nikon Digital Sight DS-Fi1 camera, Izasa, Barcelona, Spain). Ciliates were identified with the key of Foissner (1999). Cyanobacterial and diatom identification was done based on morphology focusing on species previously described for similar environments in Spain. The rest of bacterial populations were commercially analyzed using fluorescence in situ hybridization (FISH) with the VIT® gene probe technology (Vermicon, Munich, Germany). This approach deploys a set of specific oligonucleotide probes covering the main (bacteria divisions and subdivisions) bacterial phyla present in environmental samples. Hybridization and DAPI (4',6-diamidino-2-phenylindole) staining for total cell counts was carried out according to Snaidr et al. (1997). VIT® gene probe technology is based on the use of fluorescently labeled oligonucleotide probes, which specifically bind to the rRNA of living cells. Identification and quantification was performed using an Axioplan 2 fluorescence microscope (Zeiss, Oberkochen, Germany) equipped with filter sets suitable for the detection of DAPI-, 6FAM- and Cy3-related fluorescence signals and VIT® vision camera and software package (Vermicon AG, Munich, Germany). For analysis of total viable counts, the EUB probe mix (Daims et al. 1999) was used and negative controls with no probe were done. The percental area of cells per phylum in relation to the total viable area was analyzed in at least ten randomly selected captured fields, and an average percentage per bacterial phylum was calculated. No extra permeabilization for gram-positives was done as samples were ethanol-fixed.

3.3 Mineralogical Analysis

Mineral composition of the sediment and mat samples was analyzed by X-ray diffraction using a Philips PW-1710 diffractometer under monochromatic Cu-K α radiation ($\lambda=1.54060~\text{Å}$) operating at 40 kV and 30 mA, a step size of 2θ 0.02° and time per step of 2 s. Diffractograms were interpreted using EVA Bruker software. For high-resolution textural and morphometric analyses, gold-coated fresh sediment samples and samples fixed using glutaraldehyde (2.5% v/v) were scanned using a JEOL JSM-820 operating at 20 kV and equipped with an Oxford energy-dispersive X-ray microanalyzer (SEM-EDAX). Fresh pieces of non-coated sediment and mat samples and thin sections placed on sample holders supported by carbon conductive tape were scanned using FEI Inspect microscope for environmental scanning electron microscopy (ESEM), working at 30 kV and at a distance of 10 mm, operating in high-vacuum mode, and using secondary electron and backscatter detectors. The instrument used was equipped with an Oxford Analytical-Inca X-ray energy-dispersive system (EDX).



3.4 Water Analysis

Electrical conductivity (EC), temperature (T), dissolved oxygen (DO) and pH values were measured in the field using a Hanna Instruments 9828 Multiparameter meter. Water samples were collected in sterilized 2500-ml polythene bottles, stored at 4 °C, filtered (using 0.45- μ m pure cellulose acetate membrane filters) and analyzed for ions at CAI of Geological Techniques, Geological Sciences Faculty, Complutense University of Madrid, Spain, using Dionex DX 500 Ion and METROHM 940 Professional IC Vario chromatographs. The carbonate (CO₃²⁻) and bicarbonate (HCO₃⁻) ion concentrations in the water were determined by titration (Rice et al. 2012).

Water and mineralogical analysis also include some data obtained from 8 years of fieldwork.

Hydrogeochemical modeling was carried out using the PHREEQC program (Parkhurst and Appelo 1999) to calculate saturation indices with respect to the minerals found. Due to the high ionic strength of the solutions in this study, Debye–Hückle equations were not appropriate; hence, a Pitzer-salts database was used instead for all calculations.

3.5 Experimental Treatment of Excised Mat Samples

Experimental treatments were carried out in order to find the optimal conditions for mat growth. Excised pieces of microbial mats were placed in small containers ($5 \times 5 \times 5$ cm) either directly or on a thin layer of glass beads or carbonate sand at the bottom. The containers were filled with water. Three different water compositions were used: filtered lake water, Instant Ocean salts set at the appropriate salinity (i.e., mimicking the salinity of Lake Eras and Lake Altillo Chica, respectively), and Instant Ocean augmented with magnesium sulfate. Different culture media were prepared with different pH (7-10) and salt concentrations (7, 14, 21, 28 and 42 g L⁻¹) to monitor the response of the microbial community to different physicochemical conditions through time. Different light intensities (from 0 to more than $1000 \mu \text{E m}^{-2} \text{ s}^{-1}$) and temperatures (10, 20 and 50 °C) were deployed. The evaporation effect was simulated by leaving some mats to desiccate. All other mats were kept submersed at all times by adding deionized water weekly. After optimal growth conditions were determined, mats were transferred to larger containers ($10 \times 10 \times 5$ cm and larger sizes) to yield more biomass, after which some were used for experiments such as changing water chemical properties (pH, salinity, etc.) to mimic lakes cycles observed in the field. Mat development was monitored by optical microscopy (Olympus BX 51) and SEM (FEI Phenom ProX table top SEM with EDS).

3.6 Microelectrode Measurements

Microbial mat were maintained under natural light conditions in a greenhouse at 18–22 °C. Multiple microelectrode profiles of oxygen and sulfide concentrations and pH were measured in each microbial mat. The samples selected for profiling were grown on glass beads at the average salinity for each lake. The samples selected for profiling were well-developed mats, which are representing growing and decaying microbial mat stages. Microbial mats display slight variations in sedimentary features (e.g., thickness of the mineral crust, depth and thickness of the cyanobacterial layer), and therefore, representative profiles are shown (1 per lake). Replicate profiles (not shown) displayed similar patterns, with slight differences in depth and magnitude of the oxygen peak. Clark-type potentiometric oxygen



and amperometric sulfide needle electrodes with built-in guard and reference electrodes were connected to a portable picoammeter (Unisense PA 2000, Aarhus, Denmark). pH values were measured with a potentiometric needle electrode connected to a high-impedance millivolt meter (Unisense Field Microsensor Multimeter). The sensors were deployed in 100–200 µm depth increments using a manual micromanipulator (National Aperture, New Hampshire). Two replicate profiles covering the upper 10–20 mm of each mat were measured and profiles plotted using calibration curves determined before and after the measurements. A second set of profiles was measured in the early morning at sunrise to contrast noontime profiles.

Temperature and salinity were kept constant during the electrode measurements, and photosynthetically active radiation (PAR; 400–700 nm) fluctuated less than 10%. PAR was measured using a LI-COR LI 250A light meter with a LI-COR LI 190 quantum sensor (LI-COR Biosciences, Lincoln, NE, USA).

4 Results

4.1 Microbial Mat Coverage and Structure of Lake Eras and Lake Altillo Chica

Due to the ephemeral nature of the lakes, rarely completing a hydrological cycle without desiccating, mats were typically less than one centimeter in thickness. The mats extended over large areas of the lakes and even covered the entire bed of submersed areas (Fig. 2a, c). The microbial mats decayed occasionally from summer to winter (Fig. 2b, d). Direct observations in the field showed that the metabolic gases of organic matter decomposition produced sufficient buoyancy to detach parts of the benthic mats. The floating fragments were transported to the shoreline by wind. After disruption by storms, microbial mats resumed colonization of the lake bed. In the spring, during the peak development of the microbial mats in Lake Eras, a massive growth of the charophyte *Chara canescens* (Cirujano et al. 2007) was observed (Fig. 2a). The rhizoids anchored into the surface layer and protruded into microbial mats disrupting their integrity (Fig. 2a). The development of charophytes Chara galioides (Cirujano 1980) and Lamprothamnium papulosum var. toletanum (Cirujano et al. 2007) in Lake Altillo Chica was less extensive and probably did not impact the fabric of the microbial mats. During the spring, the oxygen bubbles produced during photosynthesis by cyanobacteria, diatoms, microflagellates and green algae such as Spirogyra, lifted fragmented mats to the surface of the water column, forming floating mats. Lake Eras mats were also disrupted by actively grazing micrometazoa, specifically rotifers, protist ciliates such as *Litonotus* sp., *Euplotes* sp., and some species of prostomids (Cabestrero et al. 2015b).

The microbial mats were sampled under two developmental stages. The first samples were taken in both lakes when environmental conditions supported microbial mat development (Fig. 2a, c). This was indicated by actively photosynthesizing cyanobacteria and diatoms at the surface, producing organic matter including exopolymeric substances (EPS). In these samples (designated growing microbial mat, GMM), production of organic carbon is greater than the degradation, and the greenish phototropic layer showed a great thickness of up to 2 cm. The second samples were collected in both lakes when the mats were decaying (Fig. 2b, d). Apparently, there was little or no photosynthesis (e.g., no oxygen bubbles visible) and degradation of organic matter governed (designated decaying microbial mat, DMM). Although growing and decaying stages represented extreme scenarios of microbial



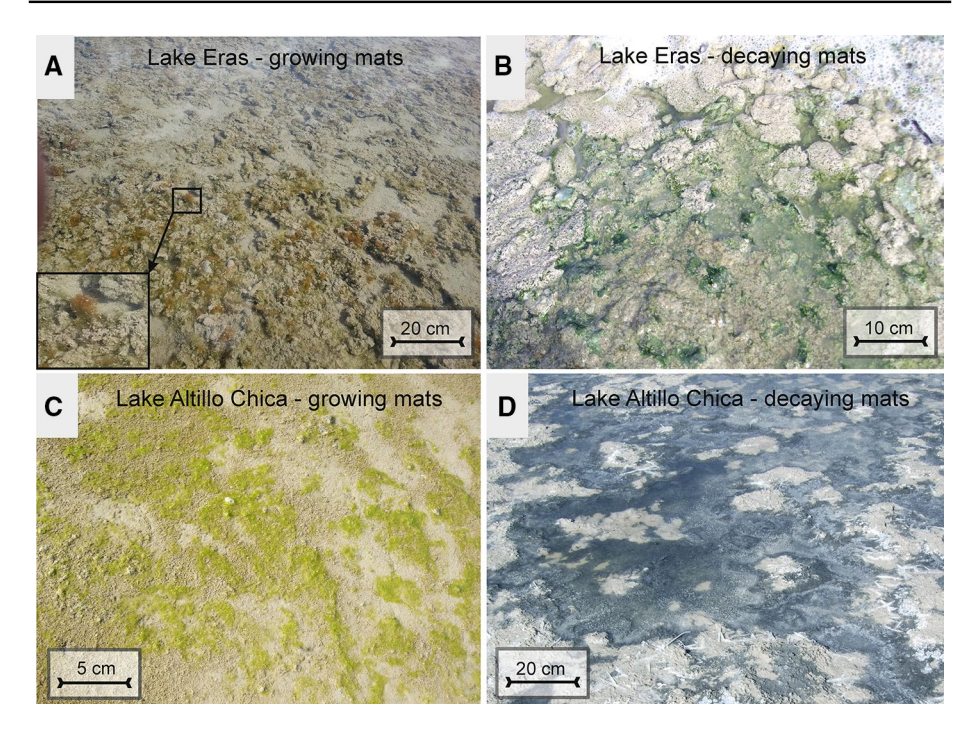


Fig. 2 Top view of the microbial mats at the time of sampling in Lake Eras (a, b) and Lake Altillo Chica (c, d). a, c Actively growing mats with green-yellowish growing mat surfaces. Note the charophytes protruding into the Lake Eras microbial mat and oxygen bubbles produced by actively photosynthesizing cyanobacteria and diatoms in Lake Altillo Chica. b, d Taken during the decaying mat stage in Lake Eras and Lake Altillo Chica, respectively. The dark-gray surface appearance indicates precipitation of carbonate and sulfate minerals

mat development and decomposition, sometimes mats showed a consecutive short growth phase (referred to as "late growing microbial mat"), during which three layers could be discerned (Fig. 3a, b): A green to golden-brown layer (1–10 mm of thickness) comprised the oxic-photic zone. Light microscopy observations revealed that this layer was dominated by blue-green cyanobacteria and yellow-brown colored diatoms (Fig. 3c). Below the previous layer, a reddish-brown transition layer ranging from 1 to 10 mm in thickness included different microorganisms (Fig. 3d), predominantly purple sulfur bacteria (identifiable by their distinctive bright sulfur granules; Fig. 3d, e), and/or purple non-sulfur bacteria (Fig. 3f). This layer also contained some unicellular cyanobacteria with a green to red appearance. The deepest layer was gray to black (ranging from 1 to 60 mm in thickness) and contained small (< 1 μ m) non-descriptive microorganisms, intermixed with the minerals and decaying organic matter. This anoxic layer had a characteristic sulfide smell produced by sulfate-reducing bacteria that remain active until the bed desiccates completely during the late spring or the summer.

4.2 Hydrochemistry and Mineralogy of Lake Eras

The environmental conditions in growing and decaying microbial mat stages showed significant differences. The air temperature was 19.0 °C during the growing stage and 7.4 °C



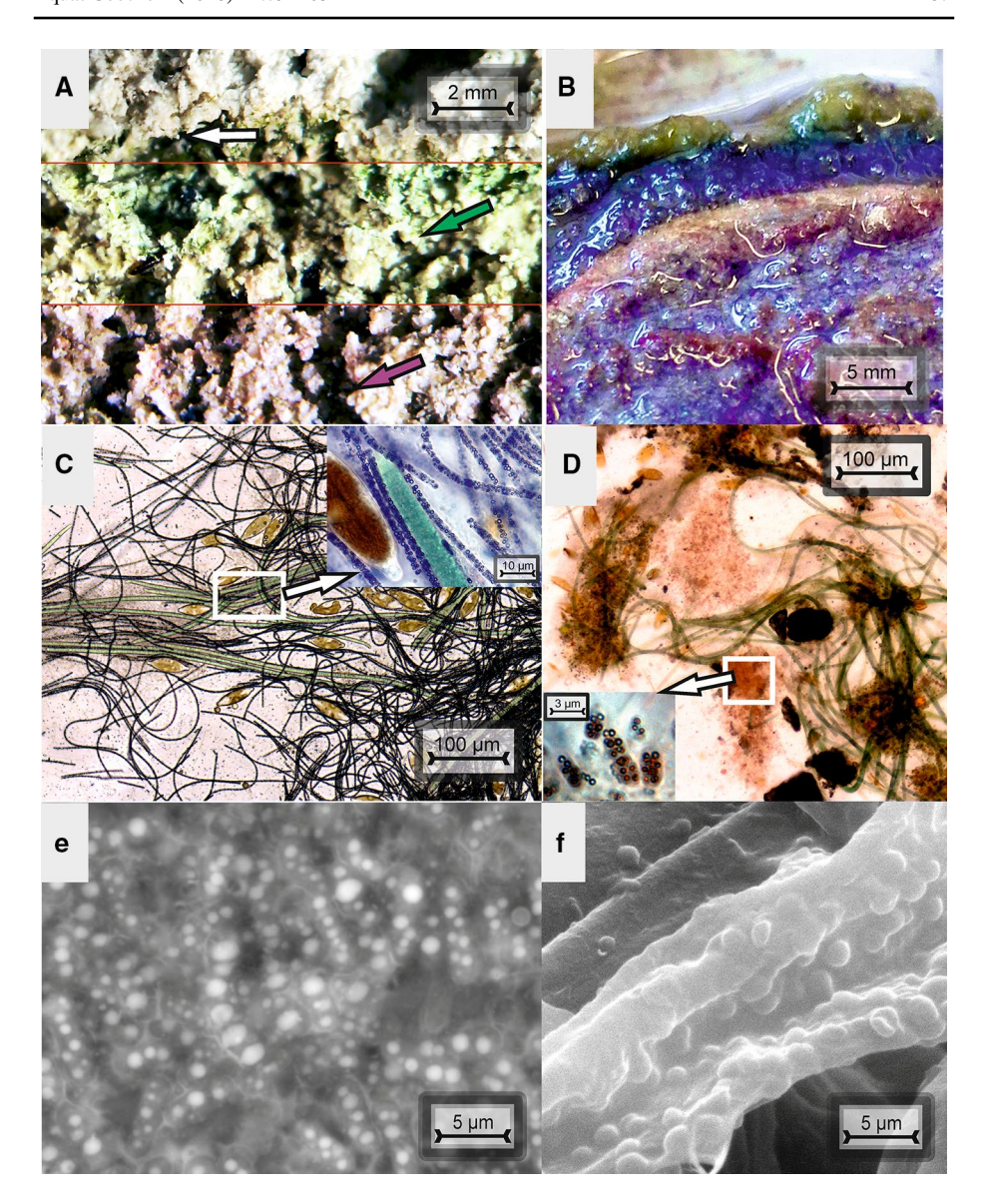


Fig. 3 Detailed view of microbial mats (close up of vertical sections) from Lake Eras (**a**) and Lake Altillo Chica (**b**). The upper 5 mm is dominated by cyanobacteria, diatoms and filamentous sulfur-oxidizing bacteria in Lake Eras (**c**). The red layer in Altillo Chica mats mainly consists of *Chromatium*-like purple sulfur bacteria (magnified ×10 in insert) and some cyanobacteria (**d**). Scanning electron micrographs showing purple sulfur bacteria with their distinctive bright sulfur granules from Lake Altillo Chica (**e**). Possibly purple non-sulfur bacteria attached to cyanobacterial filaments in Lake Eras (**f**)

during the decaying stage. The water temperature (Table 1) at noon was slightly higher than that of the air (21.9 and 8.5 °C during growing and decaying mats, respectively). The DO concentration, recorded close to the sediment surface, was 44.9% in the decaying mats, and increased to 151.3% in the actively growing mats. The pH was 10.4 during



Table 1 Water quality data of Eras and Altillo Chica corresponding to growing (GMM) and decaying (DMM) microbial mats stages: water temperature (Tw), pH, dissolved oxygen (DO), salinity (S) and oxidation-reduction potential (ORP)

| Lake | Stage | Weather | Tw (°C) | pН | DO (%) | S (%o) | ORP (mV) |
|---------------|-------|---------|---------|-------|--------|--------|----------|
| Eras | GMM | Sunny | 21.92 | 11.11 | 151.3 | 5.59 | - 61.9 |
| Eras | DMM | Rainy | 8.45 | 10.37 | 44.9 | 5.8 | - 177.1 |
| Altillo Chica | GMM | Rainy | 11.17 | 8.24 | 54.7 | 50.07 | 122.4 |
| Altillo Chica | DMM | Cloudy | 14.92 | 8.06 | 14.6 | 55.09 | 87.7 |

the decaying stage and 11.1 during the growing stage. The salinity was fairly constant: 5.6 g L⁻¹ in growing mats and 5.8 g L⁻¹ in decaying mats. The ratio of ion concentrations remained constant and corresponded to a Na⁺–Cl⁻ brine commonly observed in this basin, shown in the Piper classification (Fig. 4). Groundwater input during the winter slightly increased the water column concentration of Mg²⁺, Cl⁻ and carbonate ions. The pore water

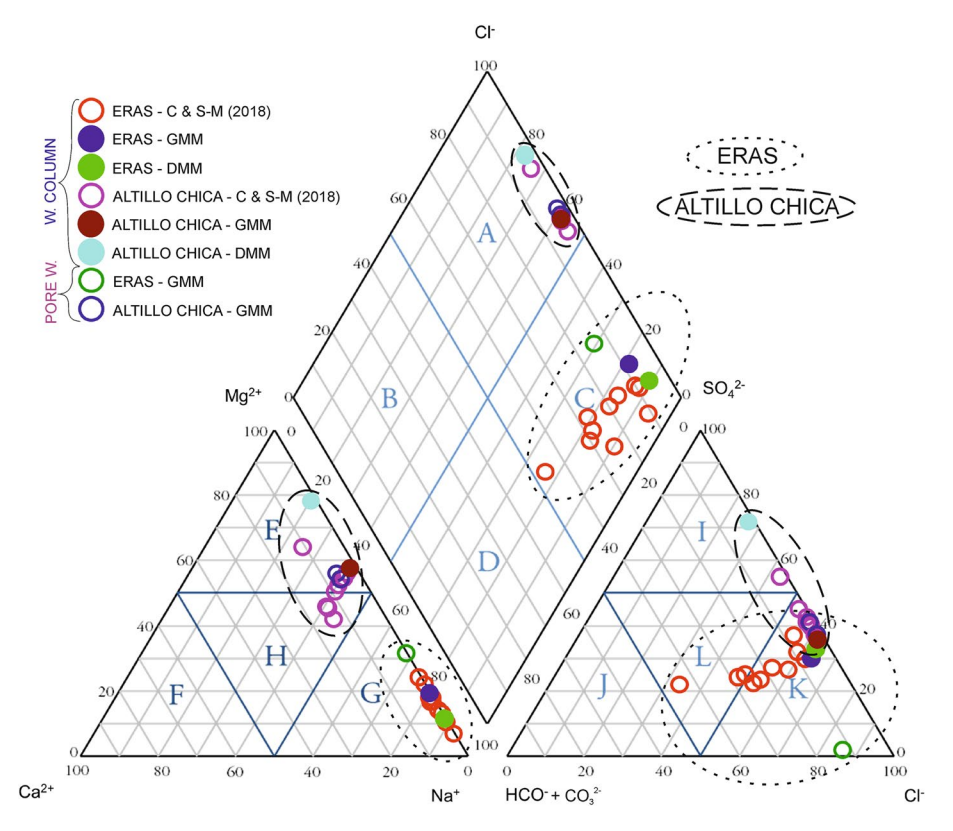


Fig. 4 Piper-Hill-Langelier diagram showing cation and anion ratios in the water column (w. column) and in the pore water (pore w.) of Lake Eras and Lake Altillo Chica. The water composition for each sampling dates is indicated in specific colored solid circles. Open circles represent hydrochemical data taken from Cabestrero and Sanz-Montero (2018). Short-dash ellipses: Lake Eras. Long-dash ellipses: Lake Altillo Chica



of the growing microbial mats was enriched in Mg²⁺, Cl⁻ and carbonate ions. A maximum depth of the lake (0.4 m) was registered.

Mineralogical analyses include one sediment sample from each lake devoid of microbial mats which was necessary to interpret the mineral composition within the mats (Fig. 5). This revealed authigenic carbonates including hydromagnesite, nesquehonite, calcite, dolomite and aragonite. Aragonite was only found in the growing microbial mat (Fig. 5a). Hydromagnesite was only present in decaying and dry mats, where it was the most abundant carbonate mineral (Fig. 5b, c). Calcite was present in all samples but its proportion increased in microbial mats (Fig. 5a, b) when compared to bare sediments devoid of mats (Fig. 5d). Dolomite was present at low concentrations associated with nesquehonite, and their presence increased in the decaying microbial mat (Fig. 5b). Minor minerals included lenticular gypsum and tabular natron crystals, both of which were more abundant in sediments devoid of microbial mats (Fig. 5d). Mg–Na sulfates and halite were found forming crusts atop of the actively growing mats (Fig. 5a).

According to modeling efforts, calcite, aragonite, dolomite and hydromagnesite were supersaturated (positive saturation indices, Table 2) both in overlying water during growing and decaying microbial mat stages. In contrast, for halite, nesquehonite and sulfates the saturation indices calculated were negative (Table 2).

4.3 Hydrochemistry and Mineralogy of Lake Altillo Chica

The water temperature of Lake Altillo Chica at noon was 11.2 and 14.9 °C during growing and decaying microbial mat stages, respectively. At the same time, the air temperature was 9.8 and 19.0 °C, respectively. Similar pH (8.1–8.2) and salinity values (50–55 g L $^{-1}$) were observed in both stages (Table 1). The DO content decreased from 54.7% in growing mats to 14.6% in decaying mats. The hydrochemistry in Lake Altillo Chica could be classified as Mg^{2+} –Cl $^-$ during the growing stage, commonly observed for surficial and interstitial water, but changed to a Mg^{2+} –SO $_4^{2-}$ -composition during the decaying stage (Fig. 4). The water column was very shallow: 4 cm deep above growing mats and 3 cm when decaying mats were present.

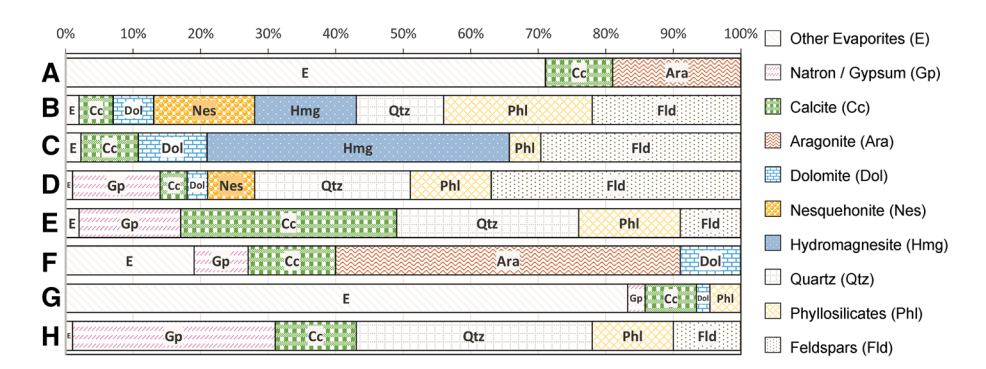


Fig. 5 Relative abundance of minerals associated with the growing microbial mats (**a**, **e**), decaying microbial mats (**b**, **f**), desiccated mats (**c**, **g**) and bare sediments devoid of microbial mats (**d**, **h**) from Lake Eras (**a**-**d**) and Lake Altillo Chica (**e**-**h**). Desiccated mat data were taken from Cabestrero and Sanz-Montero (2018)



| Lake | Eras | | Altillo Chica | | |
|----------------|--------------|---------------|---------------|---------------|--|
| Stage | Growing mats | Decaying mats | Growing mats | Decaying mats | |
| Gypsum | - 1.95 | - 1.93 | - 0.14 | 0.43 | |
| Bloedite | - 7.34 | - 7.51 | - 3.70 | - 0.21 | |
| Hexahydrite | - 3.33 | - 3.56 | - 1.62 | - 0.12 | |
| Starkeyite | - 4.25 | - 4.36 | - 2.49 | -0.78 | |
| Thenardite | - 4.49 | - 4.44 | - 2.59 | -0.78 | |
| Halite | - 4.08 | - 4.13 | - 2.31 | - 0.82 | |
| Nesquehonite | - 0.77 | - 1.35 | - 0.85 | -0.64 | |
| Calcite | 0.74 | 0.48 | 0.76 | -0.03 | |
| Aragonite | 0.54 | 0.29 | 0.56 | -0.23 | |
| Hydromagnesite | 4.14 | 2.08 | 0.07 | 3.68 | |
| Dolomite | 3.15 | 2.59 | 3.19 | 2.94 | |

Table 2 Saturation indices of the minerals commonly found in growing and decaying mats of Lake Eras and Lake Altillo Chica

Values in bold for supersaturated minerals

Lenticular gypsum crystals were observed in all samples (Fig. 5), increasing in abundance in sediments devoid of microbial mats. Calcite was also present in all of the samples and small amounts of detrital calcite were observed in bare sediments. Authigenic calcite was more abundant than detrital calcite, and the highest concentration of this mineral was found in actively growing microbial mats (Fig. 5e). Dolomite and large amounts of aragonite were found in the decaying microbial mats (Fig. 5f). Mg–Na sulfate and halite minerals comprised more than 80% of sediment surface when Lake Altillo Chica was dry (Fig. 5g). These minerals were more abundant in the microbial mats (Fig. 5e, f) than in sediments lacking microbial mats (Fig. 5h).

The saturation indices calculated indicate that during the growing microbial mat stage the solutions were supersaturated in calcite, aragonite, dolomite and hydromagnesite and undersaturated in nesquehonite (Table 2). Dolomite and hydromagnesite remained supersaturated in the decaying microbial mats while calcite, aragonite and nesquehonite were undersaturated. Halite and sulfates were undersaturated in both mat stages, except for gypsum that was supersaturated in the decaying microbial mat stage (Table 2).

4.4 Microbial Mat Community

Microscopic observations (SEM, phase contrast and DIC optical microscopy) revealed cyanobacteria and microscopic eukaryotic algae, mainly *Spirogyra*, diatoms and euglenoid flagellates (Fig. 3). These phototrophic organisms combined comprised > 60 vol% of the growing microbial mats, but only < 20 vol% in decaying microbial mats. Smaller prokaryotes (i.e., $< 5 \mu$ m) were quantified using FISH analyses (Fig. 6). The active cells comprised 65% of the total microbial cell count in growing mats and 30% in decaying mats samples of both lakes.



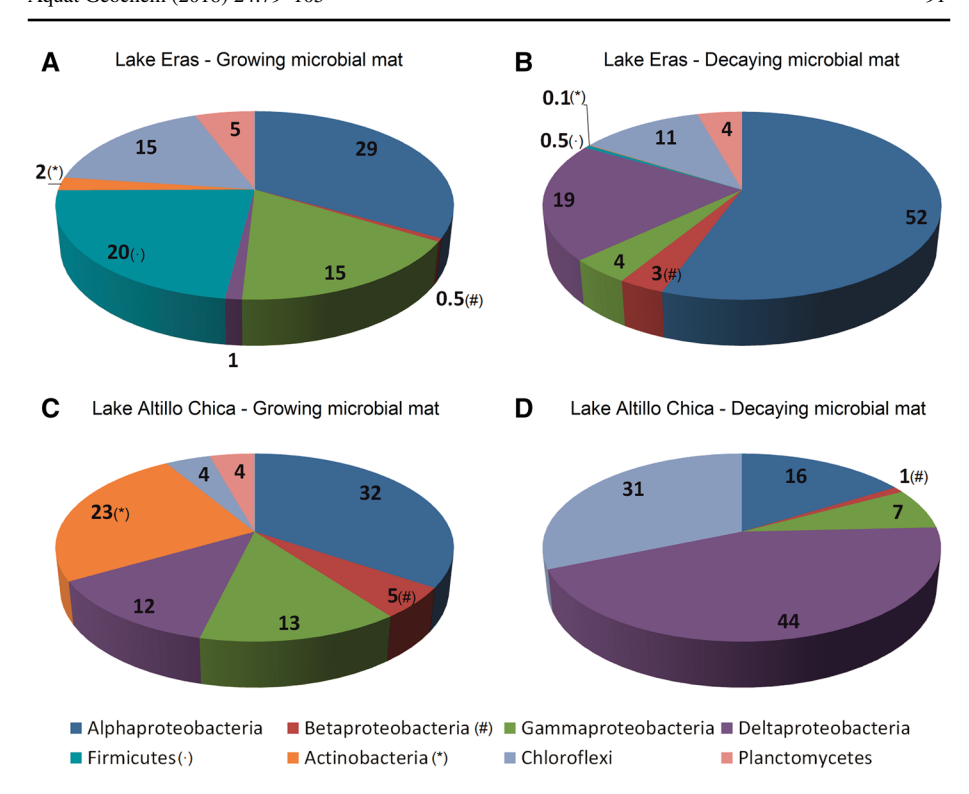


Fig. 6 Microbial diversity using FISH-VIT® gene probe technology for growing microbial mats (**a**, **c**) and decaying microbial mats (**b**, **d**). **a**, **b** Data for Lake Eras mats and **c**, **d** Results for Lake Altillo Chica mats. Microbial characterization was carried out at the level of phyla (division), except for Proteobacteria, which were analyzed at the class (subdivision) level

4.4.1 Lake Eras

Microscopy revealed that cyanobacteria, predominantly *Oscillatoria-like* (Fig. 3c) and *Phormidium-like*, and the diatoms *Aneumastus* sp. and *Navicula* sp. were the first to colonize the sediments after the winter. In the spring, during the early stage of the microbial mat growth, the pelagic filamentous green algae *Spirogyra* sp. settled from the water column onto the mat. *Chara canescens* colonized the surface of the microbial mats. The flagellate *Euglena* sp. was observed gliding through the microbial mat. Filamentous colorless sulfur bacteria (Fig. 3c) and rod-shaped purple sulfur bacteria (Fig. 3d) were commonly found below the cyanobacterial layer. Late summer desiccation triggered a massive and rapid decay of biota (decaying microbial mat stage). Patches of purple non-sulfur bacteria appeared at the surface of the mats. During the decay stage, both photosynthetic (*Nodularia spumigena* and *Anabaena* spp.) and heterotrophic (*Stanieria* spp.) cyanobacteria were present.

Four major phyla and four major classes (all belonging to the phylum Proteobacteria) were detected. Proteobacteria contributed 45.5% to the total diversity in the growing mats (Fig. 6a): Alphaproteobacteria (29%), Gammaproteobacteria (15%), Deltaproteobacteria (1%) and Betaproteobacteria (0.5%). Besides Proteobacteria, all other phyla detected contributed for 42%: Firmicutes (20%), Chloroflexi (15%), Planctomycetes (5%) and



Actinobacteria (2%). In the decaying mats, Proteobacteria comprised 78% of the total diversity (Fig. 6b) with Alphaproteobacteria (52%), Deltaproteobacteria (19%), Gammaproteobacteria (4%) and Betaproteobacteria (3%). Chloroflexi (11%), Planctomycetes (4%), Firmicutes (0.5%) and Actinobacteria (0.1%) accounted for 15.6% of total diversity. The viable microbial count was two orders of magnitude higher in growing than in decaying microbial mats. Alphaproteobacteria were the dominant group in Eras during both sampling dates and represented half of the total diversity in decaying mats. Clusters of coccoid and rod-shaped bacteria made up this class (Fig. 7a-c). Firmicutes as clusters of coccoid and rod-shaped bacteria (Fig. 7d-f) were abundant in growing mats, but they decreased in decaying mats. Deltaproteobacteria presence increased in decaying mats as coccoid clusters, and sometimes they were also identified as filaments. Chloroflexi occur as filamentous bacteria and single cells (Fig. 7g-i) with similar percentage in both microbial mats stages. Gammaproteobacteria were twice as high in growing as in decaying mats stages. Gammaproteobacteria were mainly identified as coccoid morphologies by FISH, but light microscopic observations showed that filamentous (*Beggiatoa*-like) sulfur-oxidizing bacteria were also common (Fig. 3a).

4.4.2 Lake Altillo Chica

Occasional meteoric precipitation events diluted the brine lake, after which diatoms (*Aneumastus* sp. and *Mayamaea* sp.) and cyanobacteria (*Oscillatoria* sp. and *Anabaena* sp.) rapidly increased in abundance. However, these phototrophs comprised less than 40% by volume of the total microbial community in growing microbial mats and < 10% by volume in decaying mats. When cyanobacteria colonized the sediments, other photosynthetic bacteria (e.g., purple sulfur bacteria) also occupied this ecological niche. Following desiccation, death organisms accumulated at the sediment surface of the decaying mats (Fig. 2d).

Three major phyla and four major classes belonging to the phylum Proteobacteria were detected in the growing mats of Lake Altillo Chica. Proteobacteria contributed 62% to the total diversity (Fig. 6c): Alphaproteobacteria (32%), Gammaproteobacteria (13%), Deltaproteobacteria (12%) and Betaproteobacteria (5%). Besides Proteobacteria, other three phyla detected contributed 31%: Actinobacteria (23%), Chloroflexi (4%) and Planctomycetes (4%). In the decaying microbial mats stage, Proteobacteria made up 68% of the total diversity (Fig. 6d) with Deltaproteobacteria (44%), Alphaproteobacteria (16%), Gammaproteobacteria (7%) and Betaproteobacteria (1%). Chloroflexi (31%) was the only phylum that was found in addition to the Proteobacteria in this stage. Thirty times more cells that are viable were counted in growing than in decaying microbial mats. Alphaproteobacteria consisted of coccoid cells grouped in small clusters. In contrast, Deltaproteobacteria were present as single cells or small clusters of rod-shaped cells (Fig. 7j–l). Actinobacteria comprised single or short chains of rod-shaped bacteria (Fig. 7m–o), filamentous and single cells of Chloroflexi were present, and Gammaproteobacteria were mainly coccoid cells (Fig. 7p–r). No Firmicutes were found.

4.5 Incubations of Mat Samples Under Artificial Conditions

The role of the various microbial groups in mineral precipitation was further investigated in experimental manipulations of excised mat samples using microsensors in greenhouse incubations under field conditions (e.g., of light and temperature) to determine the depth distribution of oxygen, pH and sulfide concentrations.



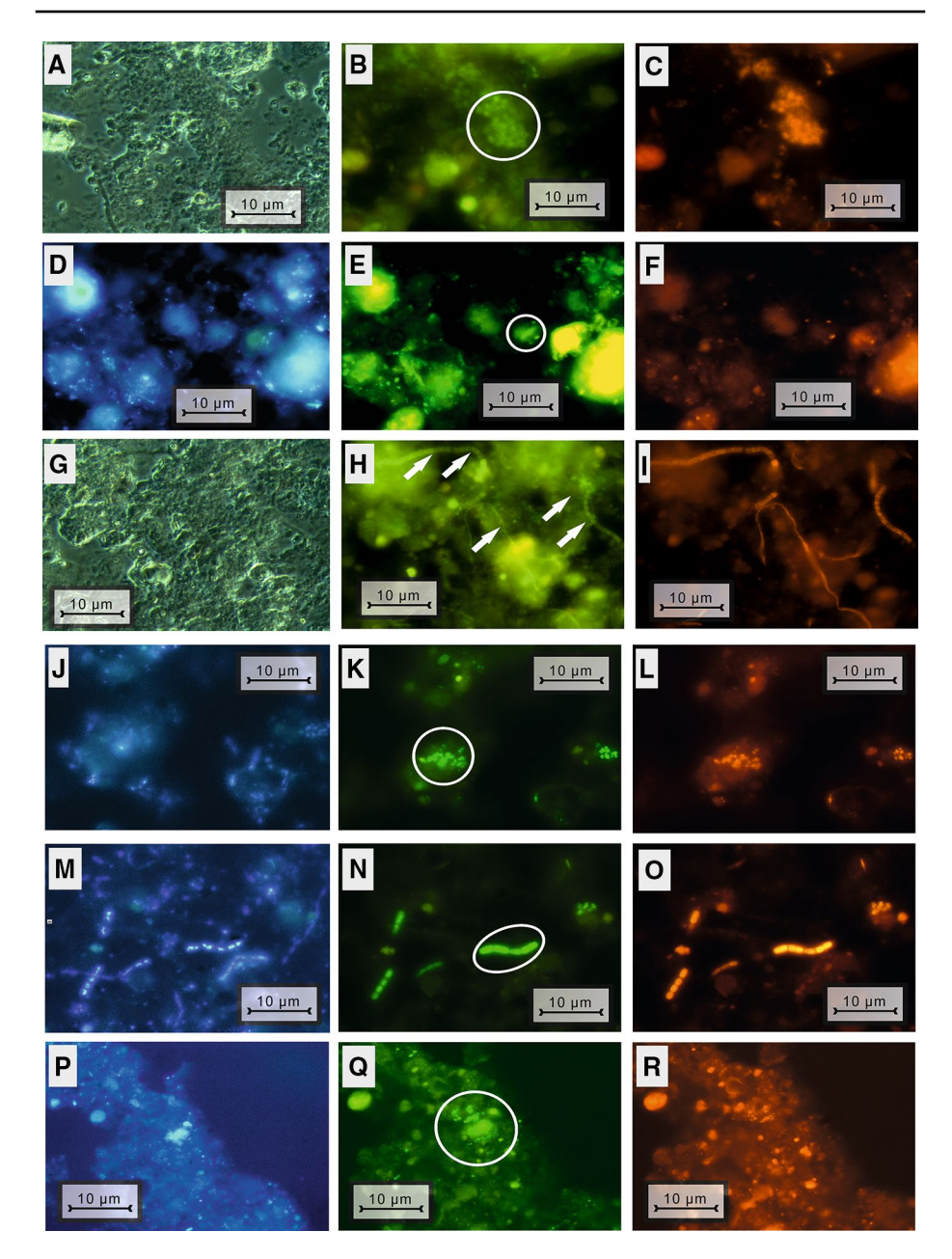


Fig. 7 Fluorescence in situ hybridization (FISH) microscopic images from Lake Eras mats (**a**–**i**) and Lake Altillo Chica mats (**j**–**r**). **a**, **g** Unstained images. **d**, **j**, **m**, **p** Stained images using DAPI (4',6-diamidino-2-phenylindole) for viable and dead bacteria (blue). Images in **b**, **e**, **h**, **k**, **n**, **q** used the general bacterial probe (green). Arrows and circles indicate organisms detected. Images in **c**, **f**, **i**, **l**, **o**, **r** were stained red with specific probes labeled with Cy3: c: Alphaproteobacterial probe; f: Firmicutes probe; i: Chloroflexi probe; l: Deltaproteobacterial probe; o: Actinobacterial probe; r: Gammaproteobacterial probe



Incubation conditions such as light intensity $(0-2000 \mu E m^{-2} s^{-1})$, temperature $(10-25 \, ^{\circ}C)$, and salinity $(0-100 \, g \, L^{-1})$ were deployed (Fig. 8a, b) and the observations showed that most cyanobacteria and diatoms thrived at a lower concentration of brine (under 50 g L^{-1}). Some of cyanobacterial species survive under almost dry conditions (*Stanieria*), while others cannot survive desiccation and/or high solar irradiation (*Oscillatoria* sp.). Microscopic observations in well-developed mats (late stage of growing

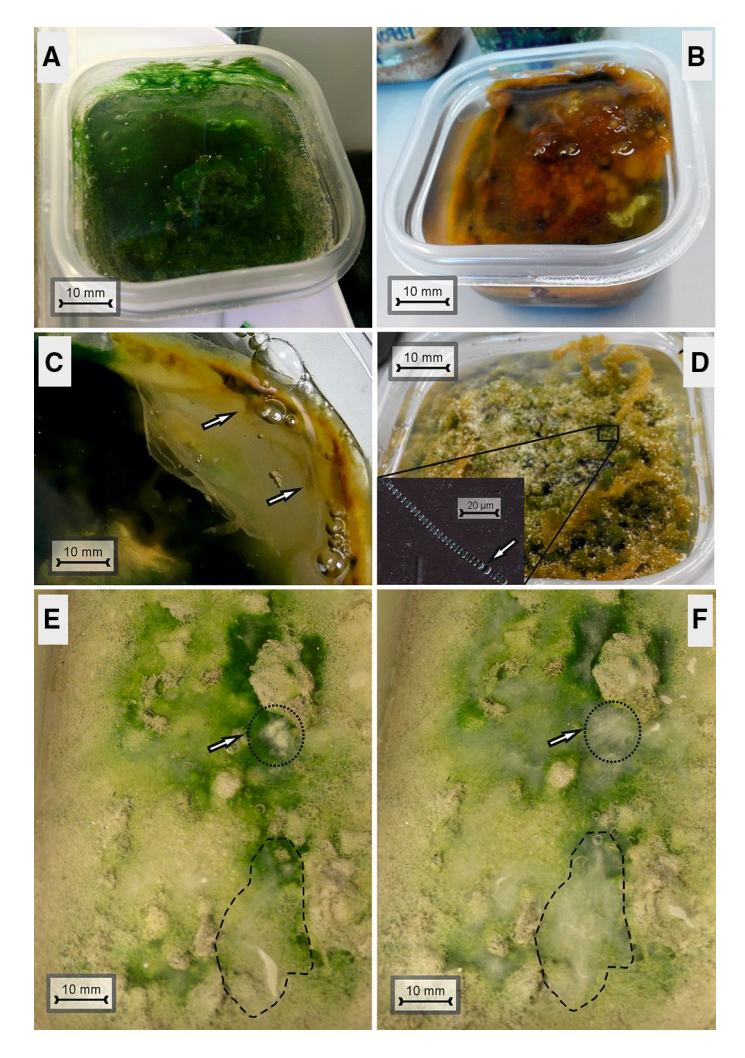


Fig. 8 Images of microbial mats from laboratory incubations from Lake Eras (a, b, e, f) and Lake Altillo Chica (c, d) showing the effects of an increase in salinity over the course of several months. This increase turned the Lake Eras mat from green (a) to orange-brown (b), which is similar to what was observed in the field. Microorganisms respond to the increase in salinity, e.g., by producing protective EPS overlying mat (c—Lake Altillo Chica mat) and/or forming specialized cells (d—Lake Eras mat) such as heterocysts, akinetes and hormogonia (Anabaena sp.). Arrows and dotted areas (white patches in e and f) show the motility of filamentous sulfur-oxidizing bacteria observed in Lake Eras mats. These organisms follow the oxygen sulfide interface, which is positioned below the mat surface during the day (e) and at the mat surface at the end of the night (f)



microbial mats) showed that the surface layer was mainly composed of dead phototropic organisms. This layer may have protected the active microbial community from solar radiation (including UV) and desiccation. The decay of the biomass in this layer possibly released organic compounds that were used by heterotrophic microbes. This surface layer, usually dark-yellow in color, may have facilitated retention of interstitial water inside the mat (Fig. 8c). When the water chemistry (for instance salinity) was altered in welldeveloped mat incubations, the combined community metabolisms changed, modifying the pH. In contrast, when the pH was kept constant, the surface appearance of microbial mats did not change. Microscopic observations showed that during desiccation, some organisms survived by developing resistive and specialized cells such as heterocysts, akinetes and hormogonia (e.g., in Anabaena sp., Figure 8d). Light and temperature increase favored the mat growth, although very high radiation (2000 μE m⁻² s⁻¹) and/or high temperature (50 °C) were deleterious. The analyzed mats also showed that development of a filamentous sulfur-oxidizing bacterial bloom required a well-developed, highly active cyanobacterial layer growing underneath (Fig. 8e). In addition, sulfur-oxidizing bacteria were moving to the surface of the mat during the night (Fig. 8f) and to the interface of O2 and sulfide in deeper layers of the mat during the day (Fig. 8e).

4.5.1 Microbial Mat Profiles from Alkaline Lake Eras

During the middle of the day, the water temperature was 22 °C, and the light intensity ranged from 1593 to 1761 μE m⁻² s⁻¹ in the greenhouse. Under these conditions, a surface O_2 concentration of 330 μM was measured (Fig. 9A). The oxygen concentration increased to a maximum of 1038 μM at 8 mm depth and decreased to 0 μM at 11.4 mm depth. The pH displayed a similar pattern, with a surface mat value of 9.37 and a peak of 9.94 at 6.8 mm depth. A maximum pH value of 9.61 was registered at 16 mm depth. No sulfide was present to a depth of 12.4 mm after which its concentration increased to approximately

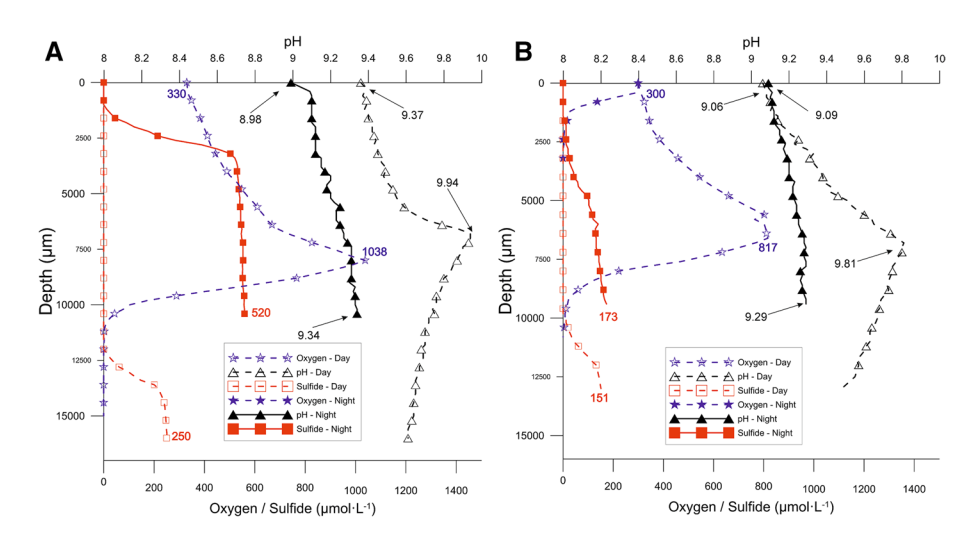


Fig. 9 Representative depth profiles of the concentration of O_2 (stars) and sulfide (squares), and pH (triangles) for Lake Eras mats (a) and Lake Altillo Chica mats (b). The microelectrode profiles were measured in mat samples under ambient light conditions in a greenhouse during peak photosynthesis between 12:00 and 14:00 (open symbols) and during the transition from dark to light between 4:30 and 6:30 (solid symbols)



 $200 \,\mu M$ at 13.6 mm depth. At greater depths, the concentration increased slightly to a maximum value of $250 \,\mu M$.

At the end of the night (e.g., at dawn), the temperature of the overlying water was 19 °C, and the light intensity varied from 45 to 89 μ E m⁻² s⁻¹ in the greenhouse. Dissolved O₂ was observed in the overlying water (not shown) but not in the mat. The pH of 8.98 at the surface increased to 9.34 at the bottom of the profile (at 10.4 mm depth). Sulfide was not detected until a depth of 1.2 mm and increased rapidly to 503 μ M at 3.2 mm. From 3.2 mm to the bottom of the profile (at 16 mm depth), the sulfide concentration continued to increase slightly to a maximum value of 559 μ M.

The salinity of the overlying water was constant with values of 11 g L^{-1} at noon, and 12 g L^{-1} at dawn.

4.5.2 Microbial Mat Profiles from the Hypersaline Lake Altillo Chica

The daytime profile, when the water temperature was 22.5 °C and the light intensity ranged from 1593 to 1761 μ E m⁻² s⁻¹ in the greenhouse, revealed a surface O₂ concentration of 300 μ M (Fig. 9b). This concentration increased to a maximum value of 817 μ M at 7 mm depth after which it decreased to 0 μ M at 11 mm depth. The pH displayed a similar pattern with a value of 9.06 at the surface of the mat and a peak of 9.81 at 7.2 mm depth. At the bottom of the profile (at 13 mm depth), a pH value of 9.48 was registered. The sulfide concentration was 0 μ M from the surface to a depth of 10.2 mm and increased to 151 μ M at 13 mm depth.

At the dawn, the profiles were measured at 19 °C, with a low light condition between 53 and 96 μE m $^{-2}$ s $^{-1}$. In contrast to the early daytime profile measured in Lake Eras mats, the Lake Altillo Chica depth profile showed dissolved O_2 , decreasing from 299 μM at the surface of the mat to 0 μM at 2.8 mm depth, respectively. In addition, the surface pH of 9.09 increased to 9.29 at 10 mm depth but did not show a peak. The sulfide concentration was 0 μM from the surface to a depth of 1.8 mm after which it increased to 173 μM at 9.8 mm. The salinity was constant at 38 g L $^{-1}$.

5 Discussion

Seasonal changes in environmental conditions, like alkalinity and salinity, play a pivotal role in the development of microbial mats (Visscher and Stolz 2005; Glunk et al. 2011; Farías et al. 2014). Fresh to brackish, alkaline water in Lake Eras supported development of thick mats, and in contrast, the higher salinity and lower alkalinity in Lake Altillo Chica produced thinner mats. The development of the two different mat types is in part determined by the local physicochemical properties, which affect the community composition, and consequently, the mineral precipitation. Each population within the mats have an specific metabolism and alter the local porewater geochemistry in a different fashion, potentially changing the saturation index. This can result in mineral precipitation or dissolution (Visscher and Stolz 2005; Dupraz et al. 2009). The combined metabolic reactions change the pH and the dissolved inorganic carbon concentration, which combined is referred to as the alkalinity engine (Dupraz et al. 2009). In addition to the alkalinity engine, the production of exopolymeric substances is also important in mineral precipitation through binding of cations and by providing mineral nucleation sites (Dupraz and Visscher 2005). Cyanobacteria are main producers of EPS, but other microbes contribute as well (Gallagher



et al. 2010; Braissant et al. 2007). We investigated the major groups of microorganisms in relation to the prevailing environmental conditions, including the physicochemistry, the organic and mineral products that comprise the mat, and we summarized this in a conceptual model contrasting the two lakes (Fig. 10). The sulfates and halides (in each lake) were not expected based on their undersaturation and because the anhydrous carbonates cannot precipitate directly from the brine (Cabestrero and Sanz-Montero 2018; Cabestrero et al. 2018; Table 2). Specifically, calcite, aragonite, dolomite and hydromagnesite only precipitated in microbial mats and not in bare sediments, even they were supersaturated in the water (Table 2).

5.1 Seasonal Evolution of the Microbial Mats

In the spring, when the Lake Eras basin started to accumulate water, growing microbial mats (Fig. 10A-1) were dominated by *Oscillatoria* sp., Alphaproteobacteria, Gammaproteobacteria and Firmicutes, and comprised small amounts of authigenic minerals including

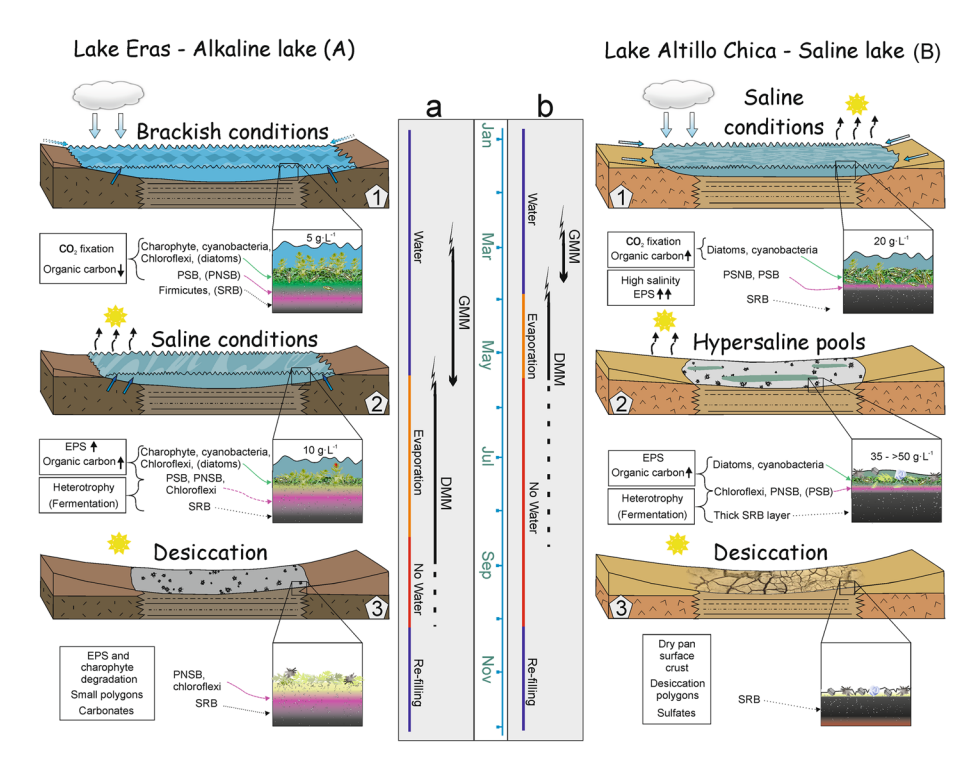


Fig. 10 A conceptual model of seasonal cycles in Lake Eras (A) and Lake Altillo Chica (B). The approximate timelines for Lake Eras (a) and Lake Altillo Chica (b) were generated from several years of observations. Three major stages are depicted from top to bottom: (1) Growing mats (GMM), during early spring, when salinity is relatively low, microbial mat development growth is rapid; (2) Early decaying mats (DMM) form during evaporation to dryness; (3) A desiccated stage of the lakes at the end of the dry season (based on continuous observations made from 2009 until 2014: Sanz-Montero et al. 2013b; Cabestrero and Sanz-Montero 2018; Cabestrero et al. 2018). Dominant groups of organisms are indicated for each stage (minor groups are listed in parentheses) for both alkaline (Lake Eras) and hypersaline (Lake Altillo Chica) sedimentary environments. Abbreviations: purple sulfur bacteria (PSB), purple non-sulfur bacteria (PNSB), sulfate-reducing bacteria (SRB) and exopolymeric substances (EPS)



calcite, aragonite and evaporites (Fig. 5). In late spring, when the water started to evaporate and the mats started to decay (early decay stage, Fig. 10A-2), the abundance of Alphaproteobacteria and Deltaproteobacteria increased whereas Firmicutes decreased and hydromagnesite, dolomite and nesquehonite precipitated. Growing mats in Lake Altillo Chica supported a community of cyanobacteria, Actinobacteria, Alphaproteobacteria, Deltaproteobacteria and Gammaproteobacteria. In this growing mat stage (Fig. 10B-1), only calcite precipitated. Deltaproteobacteria were the most abundant group in late spring (early decay stage), at the onset of desiccation and coinciding with aragonite, dolomite and evaporites formation (Fig. 10B-2). Chloroflexi were the second largest contributor to total diversity during this period.

5.1.1 Highly Alkaline Lake Conditions (Lake Eras)

Following rainfall, favorable conditions develop for colonization of the lake bed by cyanobacteria and diatoms (early stage of microbial growth) and thus presumably high rates of photosynthesis, which could explain the microbially mediated precipitation of these carbonates in late stage of microbial mat growth (Cabestrero and Sanz-Montero 2018). The metabolism of other phototrophs, such as Gammaproteobacteria and Chloroflexi, also raises the alkalinity and could promote carbonate precipitation (Visscher and Stolz 2005) in growing microbial mats, but their relatively lower abundance—as determined by FISH—suggested a minor role. High pH and high concentrations of O₂ (Fig. 9a) confirmed the activity of cyanobacteria, and microscopy revealed a dense *Oscillatoria* genus population in these well-developed mats (late stage of microbial growth). Oxygen concentrations at 8–9 mm depth peaked at > 1000 μmol L⁻¹ (Fig. 9a) and the oxic/anoxic interface was found at ca. 11 mm, indicating an important role of oxygenic phototrophy, which is typical in the upper part of mats. This metabolism is a major part in the alkalinity engine, favoring the precipitation of aragonite and calcite (Visscher et al. 1998; Dupraz and Visscher 2005).

Soda lakes typically support intense sulfur cycling (Sorokin et al. 2011). The oxidative part of the sulfur cycle (from sulfide to sulfur/sulfate) is mediated by Gammaproteobacteria (chemolithoautotrophically growing microbes: colorless sulfur-oxidizing bacteria and purple sulfur bacteria), which are commonly found in benthic mats of soda lakes (Jones et al. 1998). Elemental sulfur and sulfate minerals were found in Lake Eras mats previously (Cabestrero and Sanz-Montero 2018), and microbial sulfide oxidation may have favored their precipitation.

The relatively low abundance of sulfate-reducing bacteria in late stage of growing mats indicates that alternative organisms were involved in the reductive part of the sulfur cycle (Fig. 10A-1). Some Firmicutes have the ability to reduce sulfur, polysulfides and thiosulfate (Sorokin et al. 2012), and such sulfur compounds are commonly produced at elevated pH in mats (Visscher et al. 1992; Visscher and Van Gemerden 1993).

The abundance of Firmicutes was higher during the late stage of growing mats when compared to early stage of decaying mats; in contrast, the Alphaproteobacterial (e.g., purple non-sulfur bacteria) and Deltaproteobacterial (e.g., sulfate-reducing bacteria) contribution to total diversity increased in early stage of decaying mats. The high abundance of Firmicutes in late stage of growing mats suggests a role in the consumption of organic matter produced by photoautotrophs (predominantly charophytes, cyanobacteria and diatoms). Deltaproteobacteria (sulfate-reducing bacteria) are active throughout the mat, and their activity may peak in close proximity to cyanobacteria near the surface of the mat (Canfield and Des Marais 1991; Visscher et al. 1991, 1998; Baumgartner et al. 2006) as they thrive



in the presence of O_2 (Lefèvre et al. 2016). The sulfide profiles (showing a maximum concentration of 250–500 µmol L^{-1} ; Fig. 9a) and a sulfidic smell corroborated the activity of sulfate-reducing bacteria. H_2S produced by the sulfate reducers can diffuse to the surface of the mat and sometimes into the water column where it could support anaerobic photosynthetic metabolisms (purple sulfur bacteria, purple non-sulfur bacteria and Chloroflexi).

Alphaproteobacteria (including purple non-sulfur bacteria) were present in all mats and it increased in abundance in the decaying mats. Purple non-sulfur bacteria can grow photoautotrophically in the light or chemoheterotrophically in the dark utilizing organic compounds, hydrogen or sulfide as electron donor (Hansen and van Gemerden 1972; Madigan and Gest 1979; Imhoff 2001). They grow photoautotrophically in aerobic and anaerobic conditions but also engage in aerobic heterotrophic respiration (Madigan and Gest 1979; Drews 1981; McEwan 1994; Imhoff 2001) and may be competing with sulfate-reducing bacteria near the surface of the mat for organic carbon. Purple non-sulfur bacteria proliferate during the early stage of mat growth (Fig. 10A-1) in anoxic, reducing conditions, when ORP and DO values in the overlying water were low (Table 1). Under such conditions, these organisms grow most likely photoheterotrophically using complex organic matter (e.g., aromatic compounds and polymers including some sugars) that carried over the previous season. With increasing salinity (i.e., from late growing to early decaying microbial mat stages), the abundance of purple non-sulfur bacteria increased and that of Gammaproteobacteria (e.g., purple sulfur bacteria) decreased. This suggests that purple non-sulfur bacteria were better adapted to high salinity conditions (McEwan 1994; Navarro et al. 2009) than purple sulfur bacteria and possibly survive in concentrated brines.

The carbon pool produced by autotrophs consists of low molecular weight organic carbon and EPS or high molecular weight organic carbon (Braissant et al. 2009). Some of the low molecular weight compounds (e.g., organic acids) and EPS can bind cations in the growing microbial mats (Braissant et al. 2009; Glunk et al. 2011). In Lake Eras, groundwater is the main source of cations for the lake (Sanz-Montero et al. 2013c), specifically Mg²⁺, but Ca²⁺ is lacking (Cabestrero and Sanz-Montero 2018). This magnesium can be bound by fresh EPS (Dupraz and Visscher 2005) or low molecular weight organic carbon (Dupraz et al. 2013). Upon degradation of these organic compounds, the Mg²⁺ is released to the porewater, locally increasing the concentration. By releasing magnesium, the saturation indices of Mg carbonates increase favoring the precipitation of hydromagnesite and small amounts of dolomite in the decaying mats (Figs. 5, 10a-2). Although dolomite was supersaturated in the water column (Cabestrero and Sanz-Montero 2018), the low concentration of Ca²⁺ limited the precipitation of this Mg-Ca carbonate mineral. We propose that purple non-sulfur bacteria, sulfate-reducing bacteria and Firmicutes play a pivotal role in the degradation of organic carbon and thus in the precipitation of magnesium carbonates as their metabolisms have a proposed positive effect on the cation concentration. When the lake was completely desiccated, a red-brown layer of photoheterotrophic purple non-sulfur bacteria was present a few mm below the surface of the mat, which retained sufficient water (possibly bound to EPS) in order for the microbes to survive. The photoheterotrophic lifestyle provides a competitive advantage for purple non-sulfur bacteria over chemoheterotrophs because light is used instead of carbon as the source of energy (Madigan and Gest 1979; Hunter et al. 2008). In this final stage of growth and development (Fig. 10A-3), carbonate (i.e., hydromagnesite) precipitates throughout the mat and covers the lake surface (Sanz-Montero et al. 2013b, c; Cabestrero and Sanz-Montero 2018).

Chloroflexi were always present in significant quantities irrespective of the composition of the water. These green non-sulfur bacteria grow phototrophically with H₂ or reduced sulfur compounds as electron donor. Removal of toxic sulfide by anoxygenic phototrophs



(purple sulfur bacteria, purple non-sulfur bacteria and green non-sulfur bacteria) stimulates the growth of cyanobacteria and some heterotrophs. In addition, the filamentous morphology of Chloroflexi enhances the structural integrity of the mat. When using sulfur compounds for photosynthesis, these organisms may contribute to the alkalinity engine of the mat (Visscher and Stolz 2005; Dupraz and Visscher 2005), but the exact role of green non-sulfur bacteria in this needs further study.

5.1.2 Highly Saline Lake Conditions (Lake Altillo Chica)

Deltaproteobacteria were dominant during Lake Altillo Chica's early decaying mat stage, and Cyanobacteria, diatoms and Alphaproteobacteria were the most abundant organisms in the early growing mat stage, when the salinity was low (Fig. 10B-1). Furthermore, cyanobacteria, diatoms and Gammaproteobacteria were more abundant in growing than in decaying mats, indicating the autotrophic potential in the developing mats (Fig. 10B). Depth profiles of oxygen (maximum 817 μ mol L⁻¹ at 7 mm depth) and pH (maximum 9.81 at 7.2 mm depth) confirmed a high rate of CO₂ fixation. Microscopy suggested that the genus Oscillatoria was the main carbon fixer. The thickness of the cyanobacterial layer occasionally exceeded 10 mm in well-developed Lake Altillo Chica mats (Fig. 8c). However, due to the high salinity and the ephemeral nature of the lake, the microbial mats were typically only a few mm thick (Fig. 9b). Cyanobacteria and diatoms were more abundant than purple sulfur bacteria and green non-sulfur bacteria, indicating that the former were the main components of the alkalinity engine and thus the main mediators of carbonate precipitation in growing microbial mats. The period of active photosynthesis and mat growth ended when water started to evaporate. In dry areas of the lake bed, salt precipitation was visible (white crystals, Fig. 2d), but in some other submersed areas, mats remained intact with little or no photosynthesis and presumably high rates of heterotrophic activity. A decrease in DO and pH measured in the water column and a pungent smell supported the assumption of little or no carbon fixation and high rates of aerobic and anaerobic heterotrophy, producing fatty acids. During the early stage of mats decay, sulfate-reducing bacteria thrived, replacing Alphaproteobacteria. A high metabolic activity of sulfate-reducing bacteria was found between 35 and 195 g L⁻¹ near the surface of subtropical microbial mats subjected to a salinity cycle similar to Lake Altillo Chica (Visscher et al. 2010). A Deltaproteobacterial dominance was also reported in Tirez Lake, an ephemeral system with similar properties and in close proximity to Lake Altillo Chica (Montoya et al. 2013). Depending on the organic carbon source used as electron donor, sulfate-reducing bacteria can support carbonate precipitation in mats (Baumgartner et al. 2006; Gallagher et al. 2012). This may have favored the precipitation of aragonite and smaller amounts of calcite and dolomite in Lake Altillo Chica (Fig. 5).

Precipitation of evaporites was observed during desiccation (the late microbial decay stage), but could not be explained by the concentration of ions in the water column. Modeling efforts of water composition (Cabestrero and Sanz-Montero 2018; Cabestrero et al. 2018; Table 2) indicated that another source of ions (Na⁺, Mg²⁺ and SO₄²⁻) was needed. Presumably, cations were released during decomposition of EPS, and additional sulfates were produced during microbial and/or chemical oxidation of sulfides allowing these evaporites to form.

Sporadically, celestine crystals (< 5%) were found embedded in the late stage of microbial mats growth (Sanz-Montero et al. 2015a, b) and could have precipitated upon lysis of cyanobacteria, diatoms or green algae, as these organisms are known to sequester Ba and



Sr (Krejci et al. 2011; Cam et al. 2016). Alphaproteobacteria, and especially the Actinobacteria, which were present in late stage of microbial growth but absent in the early stage of microbial decay (Fig. 10B-1, 2) could have been involved in initial EPS degradation (Figs. 6, 10B) as their heterotrophic metabolisms can break down these polymers (Imhoff 2001; Manivasagan et al. 2013). This could explain the bloom of sulfate-reducing bacteria in early stage of microbial decay, as these organisms rely on low molecular weight organic carbon produced by partial polymer degradation (Widdel et al. 1983; Visscher et al. 2010).

Increasing salinity caused a clear shift in community composition (Fig. 6). As explained above, this was further illustrated by an increase of Chloroflexi in decaying microbial mats. These green non-sulfur bacteria are adapted to grow and survive at elevated salinity (Nübel et al. 2001). The exact role of Chloroflexi in mats remains unclear, but their mixotrophic lifestyle represents an advantage for the conditions typically found in ephemeral mats (Klatt et al. 2013).

5.1.3 Comparison of Mineral Precipitation in Lake Eras and Lake Altillo Chica Mats

As outlined above, the precipitation of minerals is mediated by the alkalinity engine, which is determined by the combined metabolisms of the entire microbial community (Gallagher et al. 2014), as well as by the properties of EPS (Dupraz et al. 2009). In both Lake Eras and Lake Altillo Chica, carbonates precipitated in growing mats. In addition, decaying Lake Eras mats supported massive hydromagnesite precipitation.

Cyanobacteria developed to a greater extent in Lake Eras than in Lake Altillo Chica, as the oxygen maximum is slightly higher in Lake Eras than Lake Altillo Chica (3.7 and 2.9 times air saturation, respectively). However, concentration profiles result from O₂ production and consumption and we interpret the absence of oxygen in Lake Eras during the night as an indication that a substantial oxygen consumption rate (i.e., aerobic heterotrophic activity) must have occurred (assuming a small contribution from chemical O2 consumption and loss through flux out of the mat). As a result, a much smaller aerobic respiration rate is assumed for Lake Altillo Chica mats, which thus have a slightly stronger "aerobic" alkalinity engine than Lake Eras does. In addition, the sulfate-reducing bacterial population was larger in Lake Altillo Chica than in Lake Eras and the maximum sulfide concentrations in both lakes suggests a lower sulfide consumption in Lake Eras. It should be noted that sulfide oxidation by colorless sulfur bacteria counteracts the alkalinity engine (Visscher and Stolz 2005). However, if purple non-sulfur bacteria, purple sulfur bacteria and green non-sulfur bacteria consume a significant fraction of the sulfide (and/or intermediate sulfur compounds such as thiosulfate and polysulfides), the overall effect of sulfide oxidation on the alkalinity engine could be different. As outlined above, we attribute a major role in the alkalinity engine to purple non-sulfur bacteria in Lake Eras. The role of these photoheterotrophs on the alkalinity depends on their metabolism (electron donor: H₂, organic carbon, reduced sulfur compounds) and could either favor carbonate precipitation or dissolution. Based on the microbial production and consumption of oxygen and sulfide assumed from the depth profiles, we attribute a stronger "anaerobic" alkalinity engine to Lake Eras. The maximum pH values were higher during the day (9.94 in Lake Eras vs. 9.81 in Lake Altillo Chica, and at the mat surface 9.37 in Lake Eras and 9.06 in Lake Altillo Chica). The minimum pH values remained similar between day and night in Lake Altillo Chica (9.06 and 9.09, respectively), but differed highly in Lake Eras (9.37 and 8.98 during the day and night, respectively). Slightly higher maximum pH values and greater differences of pH in Lake Eras versus Lake Altillo Chica suggest a slightly stronger alkalinity engine in Lake Eras.



Sulfide minerals were not observed in any sample although they are commonly present in environments where sulfate-reducing bacteria thrive (Lefèvre et al. 2016), especially microbial mats (Visscher and Van Gemerden 1993; Luther et al. 2001). A possible explanation could be a low concentration of minerals containing metals (e.g., iron) in the detrital sediments that the lakes receive and the nature of these minerals to be weathering resistant. Additionally, metals that slowly release during weathering could have been incorporated into authigenic clays (Del Buey et al. 2018). Furthermore, the biotic and abiotic oxidation of biogenic sulfide yielding intermediate sulfur compounds (e.g., polysulfides, polythionates and thiosulfate; Luther et al. 2001) could also have slowed the precipitation of sulfide minerals.

In microbial incubations, copious amounts of EPS were produced (Fig. 8a–d), showing the potential of exopolymeric production in mats from both lakes under quiescent conditions. Incubations of Lake Altillo Chica mats grew substantially thicker than Lake Eras mats (ca. 20–50 mm and less than 10 mm for Lake Altillo Chica and Lake Eras, respectively) and thus could have contained more EPS, potentially inhibiting precipitation. Extensive measurements of EPS properties were beyond the scope of this investigation, but inspection of hand samples (e.g., Fig. 3a, b) suggested that Lake Altillo Chica mats contained more EPS than Lake Eras mats.

More carbonates were present in growing and decaying mats in Lake Eras than in similar mats in Lake Altillo Chica (Cabestrero and Sanz-Montero 2018; Fig. 2). Furthermore, decaying mats in Lake Eras supported hydromagnesite precipitation (Fig. 5). We attribute this to a combination of a stronger alkalinity engine, a greater EPS availability for heterotrophic degradation and the different water composition in Lake Eras.

6 Conclusions

A study of two ephemeral lakes located in areas with a similar climate but differences in water input (groundwater in Lake Eras, meteoric precipitation in Lake Altillo Chica), alkalinity and lithology showed different microbial community compositions and consequently resulting in different alkalinity engines (a stronger anaerobic alkalinity engine in Lake Eras and stronger aerobic alkalinity engine in Lake Altillo Chica). The specific physicochemical properties of the porewater and depth of the water column, both of which were subject to vast seasonal fluctuations, were likely the major drivers in determining the community composition. Furthermore, the contrasting populations produced and consumed different amounts of EPS, which in combination with the different alkalinity engines, resulted in different mineral precipitation patterns (initially precipitation of sulfates followed by extensive carbonate mineral production in Lake Eras vs. the precipitation of carbonates followed by sulfate minerals in Lake Altillo Chica).

Acknowledgements This research work has been funded by the Spanish Ministry of Economy and Competivity, National Project CGL2015-66455-R (MINECO-FEDER). We wish to thank all the members of Project CGL2015-66455-R for their assistance. We wish to thank Claudia Beimfohr from Vermicon for clarifying the FISH analyses. We appreciate the time and effort of the Editor George Luther and three anonymous referees whose contributions improved this manuscript. This publication is part of the Scientific Activities of Research Group UCM-910404. PTV acknowledges support from NSF-EAR award 1561173. The authors declare no conflict of interest.



References

- Baumgartner LK, Reid RP, Dupraz C, Decho AW, Buckley DH, Spear JR, Visscher PT (2006) Sulfate reducing bacteria in microbial mats: changing paradigms, new discoveries. Sed Geol 185(3-4):131-145
- Braissant O, Decho AW, Dupraz C, Glunk C, Przekop KM, Visscher PT (2007) Exopolymeric substances of sulfate-reducing bacteria: interactions with calcium at alkaline pH and implication for formation of carbonate minerals. Geobiology 5(4):401–411
- Braissant O, Decho AW, Przekop KM, Gallagher KL, Glunk C, Dupraz C, Visscher PT (2009) Characteristics and turnover of exopolymeric substances in a hypersaline microbial mat. FEMS Microbiol Ecol 67(2):293–307
- Cabestrero Ó, Sanz-Montero ME (2018) Brine evolution in two inland evaporative environments: influence of microbial mats in mineral precipitation. J Paleolimnol 59(2):139–157
- Cabestrero Ó, García del Cura MA, Sanz-Montero ME (2013) Precipitación de sales en una laguna sulfatada magnésico-sódica (Lillo, Toledo): controles ambientales. Macla 17:27–28
- Cabestrero O, Sanz-Montero ME, García del Cura MA (2014a) Precipitation of magnesium bearing-sulphates in saline lakes: influence of sedimentary structures and microbial processes. In: 19th international sedimentological congress 2014, Geneva, Switzerland, pp 18–22
- Cabestrero O, Arroyo-Rey X, García del Cura MA, Sanz-Montero ME (2014b) Formación de arcillas en lagunas sulfatadas efímeras (Lillo, Toledo). Macla 19:1–2
- Cabestrero Ó, Sanz-Montero ME, Martin D (2015a) The behavior of the calcium ion in saline and alkaline lake complexes revealed by statistical techniques. U.S. Geological Survey Open-File Report 2015, 1092:42–43
- Cabestrero Ó, Arregui L, Sanz-Montero ME, Serrano S (2015b) Biodiversity of protists and prokaryotes of two playa-lakes from Central Spain. In: Abstract book: VII European Congress of Protistology, Seville, Spain
- Cabestrero Ó, Del Buey P, Sanz-Montero ME (2018) Biosedimentary and geochemical constraints on the precipitation of mineral crusts in shallow sulphate lakes. Sed Geol 366:32–46
- Cam N, Benzerara K, Georgelin T, Jaber M, Lambert JF, Poinsot M, Cordier L (2016) Selective uptake of alkaline earth metals by cyanobacteria forming intracellular carbonates. Environ Sci Technol 50(21):11654–11662
- Canfield DE, Des Marais DJ (1991) Aerobic sulfate reduction in microbial mats. Science 251(5000):1471
 Cirujano S (1980) Las lagunas manchegas y su vegetación. I. Anales del Jardín Botánico de Madrid 37(1):155–192
- Cirujano S, García P, Meco A, Fernández R (2007) Los carófitos ibéricos. Anales del Jardín Botánico de Madrid 64:87–102
- Daims H, Bruhl A, Amann R, Schleifer KH, Wagner M (1999) The domain-specific probe EUB338 is insufficient for the detection of all Bacteria: development and evaluation of a more comprehensive probe set. Syst Appl Microbiol 22(3):434–444
- Del Buey P, Cabestrero Ó, Arroyo X, Sanz-Montero ME (2018) Microbially induced Palygorskite-Sepiolite authigenesis in modern hypersaline lakes (Central Spain). Appl Clay Sci. https://doi.org/10.1016/j.clay.2018.02.020
- Drews G (1981) Rhodospirillum salexigens, spec. nov., an obligatory halophilic phototrophic bacterium. Arch Microbiol 130(4):325–327
- Dupraz C, Visscher PT (2005) Microbial lithification in marine stromatolites and hypersaline mats. Trends Microbiol 13(9):429-438
- Dupraz C, Reid RP, Braissant O, Decho AW, Norman RS, Visscher PT (2009) Processes of carbonate precipitation in modern microbial mats. Earth Sci Rev 96(3):141–162
- Dupraz C, Fowler A, Tobias C, Visscher PT (2013) Stromatolitic knobs in Storr's Lake (San Salvador, Bahamas): a model system for formation and alteration of laminae. Geobiology 11(6):527–548
- Farías ME, Contreras M, Rasuk MC, Kurth D, Flores MR, Poiré DG, Visscher PT (2014) Characterization of bacterial diversity associated with microbial mats, gypsum evaporites and carbonate microbialites in thalassic wetlands: Tebenquiche and La Brava, Salar de Atacama, Chile. Extremophiles 18(2):311–329
- Fernandez-Galiano D (1976) Silver impregnation of ciliated protozoa: procedure yielding good results with the pyridinated silver carbonate method. Trans Am Microsc Soc 95(4):557–560
- Foissner W (1999) Soil protozoa as bioindicators: pros and cons, methods, diversity, representative examples. Agr Ecosyst Environ 74(1–3):95–112
- Foster IS, King PL, Hyde BC, Southam G (2010) Characterization of halophiles in natural $MgSO_4$ salts and laboratory enrichment samples: astrobiological implications for Mars. Planet Space Sci 58(4):599–615



- Gallagher KL, Dupraz C, Braissant O, Norman RS, Decho AW, Visscher PT (2010) Mineralization of sedimentary biofilms: modern mechanistic insights. In: William CB (ed) Biofilms: formation, development and properties. Nova Science Publishers, Inc., New York, pp 227–258
- Gallagher KL, Kading T, Braissant O, Dupraz C, Visscher PT (2012) Inside the alkalinity engine: the role of electron donors in the organomineralization potential of sulfate-reducing bacteria. Geobiology 10:518–530
- Gallagher KL, Dupraz C, Visscher PT (2014) Two opposing effects of sulfate reduction on carbonate precipitation in normal marine, hypersaline, and alkaline environments: COMMENT. Geology 42(1):e313–e314
- Glunk C, Dupraz C, Braissant O, Gallagher KL, Verrecchia EP, Visscher PT (2011) Microbially mediated carbonate precipitation in a hypersaline lake, big pond (Eleuthera, Bahamas). Sedimentology 58(3):720–736
- Hansen TA, van Gemerden H (1972) Sulfide utilization by purple nonsulfur bacteria. Arch Mikrobiol 86(1):49–56
- Hunter CN, Daldal F, Thurnauer MC, Beatty JT (2008) The purple phototrophic bacteria. Springer, Amsterdam
- Imhoff JF (2001) True marine and halophilic anoxygenic phototrophic bacteria. Arch Microbiol 176(4):243–254
- Jones BE, Grant WD, Duckworth AW, Owenson GG (1998) Microbial diversity of soda lakes. Extremophiles 2(3):191–200
- Klatt CG, Liu Z, Ludwig M, Kühl M, Jensen SI, Bryant DA, Ward DM (2013) Temporal metatranscriptomic patterning in phototrophic Chloroflexi inhabiting a microbial mat in a geothermal spring. ISME J 7(9):1775–1789
- Krejci MR, Wasserman B, Finney L, McNulty I, Legnini D, Vogt S, Joester D (2011) Selectivity in biomineralization of barium and strontium. J Struct Biol 176(2):192–202
- Lefèvre CT, Howse PA, Schmidt ML, Sabaty M, Menguy N, Luther GW III, Bazylinski DA (2016) Growth of magnetotactic sulfate-reducing bacteria in oxygen concentration gradient medium. Environ Microbiol Rep 8(6):1003–1015
- Luther GW III, Glazer BT, Hohmann L, Popp JI, Taillefert M, Rozan TF, Brendel PJ, Theberge SM, Nuzzio DB (2001) Sulfur speciation monitored in situ with solid state gold amalgam voltammetric microelectrodes: polysulfides as a special case in sediments, microbial mats and hydrothermal vent waters. J Environ Monit 3(1):61–66
- Madigan MT, Gest H (1979) Growth of the photosynthetic bacterium Rhodopseudomonas capsulata chemoautotrophically in darkness with H₂ as the energy source. J Bacteriol 137(1):524–530
- Manivasagan P, Venkatesan J, Sivakumar K, Kim SK (2013) Marine actinobacterial metabolites: current status and future perspectives. Microbiol Res 168(6):311–332
- McEwan AG (1994) Photosynthetic electron transport and anaerobic metabolism in purple nonsulfur phototrophic bacteria. Antonie Van Leeuwenhoek 66(1):151–164
- Montoya L, Vizioli C, Rodríguez N, Rastoll MJ, Amils R, Marin I (2013) Microbial community composition of Tirez lagoon (Spain), a highly sulfated athalassohaline environment. Aquat Biosyst 9(1):19
- Navarro JB, Moser DP, Flores A, Ross C, Rosen MR, Dong H, Hedlund BP (2009) Bacterial succession within an ephemeral hypereutrophic mojave desert Playa Lake. Microb Ecol 57(2):307–320
- Newman DK, Banfield JF (2002) Geomicrobiology: how molecular-scale interactions underpin biogeochemical systems. Science 296(5570):1071–1077
- Nübel U, Bateson MM, Madigan MT, Kühl M, Ward DM (2001) Diversity and distribution in hypersaline microbial mats of bacteria related to Chloroflexus spp. Appl Environ Microbiol 67(9):4365–4371
- Parkhurst DL, Appelo C (1999) User's guide to PHREEQC (version 2). A computer program for speciation, batch-reaction, one-dimensional transport, and inverse geochemical calculations. U.S. Geological Survey Water-Resources Investigations Report 99(4259)
- Power IM, Wilson SA, Thom JM, Dipple GM, Southam G (2007) Biologically induced mineralization of dypingite by cyanobacteria from an alkaline wetland near Atlin, British Columbia, Canada. Geochem Trans 8(1):13
- Rice EW, Bridgewater L, Federation WE, Association APH (2012) Standard methods for the examination of water and wastewater. American Public Health Association (APHA), Washington, DC
- Rodríguez-Aranda JP, Sanz-Montero ME (2015) Tapices microbianos: los organismos que fabrican estromatolitos. Enseñanza de las Ciencias de la Tierra 23(2):208–219
- Sanz-Montero ME, Rodríguez-Aranda JP (2013) The role of microbial mats in the movement of stones on playa lake surfaces. Sed Geol 298:53–64



- Sanz-Montero ME, Calvo JP, Garcia del Cura MA, Ornosa C, Outerelo R, Rodríguez-Aranda JP (2013a) The rise of the diptera-microbial mat interactions during the Cenozoic: consequences for the sedimentary record of saline lakes. Terra Nova 25(6):465–471
- Sanz-Montero ME, Arroyo X, Cabestrero Ó, Calvo JP, Fernández-Escalante E, Fidalgo C, Rodríguez-Aranda JP (2013b) Procesos de sedimentación y biomineralización en la laguna alcalina de las Eras (Humedal Coca-Olmedo). Geogaceta 53:97–100
- Sanz-Montero ME, Cabestrero Ó, Rodríguez-Aranda JP (2013c) Hydromagnesite precipitation in microbial mats from a highly alkaline lake, Central Spain. Miner Mag 77–5:2628
- Sanz-Montero ME, Cabestrero Ó, Rodríguez-Aranda JP (2015a) Sedimentary effects of flood-producing windstorms in playa lakes and their role in the movement of large rocks. Earth Surf Process Landf 40(7):864–875
- Sanz-Montero ME, Cabestrero Ó, Rodríguez-Aranda JP (2015b) Gypsum microbialites and mat-related structures in shallow evaporitic lakes. Geological Survey Open-File Report 2015, 1092:189–190
- Sanz-Montero ME, Cabestrero Ó, Rodríguez-Aranda JP (2016) Comments on Racetrack playa: rocks moved by wind alone. Aeol Res 20:196–197
- Schneider D, Arp G, Reimer A, Reitner J, Daniel R (2013) Phylogenetic analysis of a microbialite-forming microbial mat from a hypersaline lake of the Kiritimati Atoll, Central Pacific. PLoS One 8(6):e66662
- Snaidr J, Amann R, Huber I, Ludwig W, Schleifer KH (1997) Phylogenetic analysis and in situ identification of bacteria in activated sludge. Appl Environ Microbiol 63(7):2884–2896
- Sorokin DY, Kuenen JG, Muyzer G (2011) The microbial sulfur cycle at extremely haloalkaline conditions of soda lakes. Front Microbiol 2:44
- Sorokin D, Tourova T, Sukhacheva M, Muyzer G (2012) Desulfuribacillus alkaliarsenatis gen. nov. sp. nov., a deep-lineage, obligately anaerobic, dissimilatory sulfur and arsenate-reducing, haloalkaliphilic representative of the order Bacillales from soda lakes. Extremophiles 16(4):597–605
- Visscher PT, Stolz JF (2005) Microbial mats as bioreactors: populations, processes, and products. Palaeogeogr Palaeoclimatol Palaeoecol 219(1):87–100
- Visscher PT, van Gemerden H (1993) Sulfur cycling in laminated marine microbial ecosystems. In: Oremland RTS (ed) Biogeochemistry of global change. Springer, Amsterdam, pp 672–690
- Visscher PT, Beukema J, van Gemerden H (1991) In situ characterization of sediments: measurements of oxygen and sulfide profiles with a novel combined needle electrode. Limnol Oceanogr 36(7):1476–1480
- Visscher PT, Prins RA, van Gemerden H (1992) Rates of sulfate reduction and thiosulfate consumption in a marine microbial mat. FEMS Microbiol Lett 86(4):283–293
- Visscher PT, Reid RP, Bebout BM, Hoeft SE, Macintyre IG, Thompson JA (1998) Formation of lithified micritic laminae in modern marine stromatolites (Bahamas): the role of sulfur cycling. Am Miner 83(11):1482–1493
- Visscher PT, Dupraz C, Braissant O, Gallagher KL, Glunk C, Casillas L, Reed RE (2010) Biogeochemistry of carbon cycling in hypersaline mats: linking the present to the past through biosignatures. In: Seckbach J, Oren A (eds) Microbial mats. Springer, Amsterdam, pp 443–468
- Widdel F, Kohring GW, Mayer F (1983) Studies on dissimilatory sulfate-reducing bacteria that decompose fatty acids. Arch Microbiol 134(4):286–294
- Wong HL, Smith DL, Visscher PT, Burns BP (2015) Niche differentiation of bacterial communities at a millimeter scale in Shark Bay microbial mats. Sci Rep 5:15607
- Yang J, Ma LA, Jiang H, Wu G, Dong H (2016) Salinity shapes microbial diversity and community structure in surface sediments of the Qinghai-Tibetan Lakes. Sci Rep 6:25078

